EJN fens EUROPEAN JOURNAL OF NEUROSCIENCE

European Journal of Neuroscience, Vol. 39, pp. 419–434, 2014 doi:10.1111/ejn.12470

Heterogeneous presynaptic distribution of monoacylglycerol lipase, a multipotent regulator of nociceptive circuits in the mouse spinal cord

Eszter Horváth,[1,*] Stephen G. Woodhams,[1,*] Rita Nyilas,[1] Christopher M. Henstridge,[1] Masanobu Kano,[2] Kenji Sakimura,[3] Masahiko Watanabe[4] and István Katona[1]

[1]Momentum Laboratory of Molecular Neurobiology, Institute of Experimental Medicine, Hungarian Academy of Sciences, Szigony utca 43., H-1083 Budapest, Hungary

[2]Department of Neurophysiology, Graduate School of Medicine, University of Tokyo, Tokyo, Japan

[3]Department of Cellular Neurobiology, Brain Research Institute, Niigata University, Niigata, Japan

[4]Department of Anatomy, Hokkaido University School of Medicine, Sapporo, Japan

Keywords: endocannabinoid, MAGL, monoglyceride lipase, pain, prostaglandin

Abstract

Monoacylglycerol lipase (MGL) is a multifunctional serine hydrolase, which terminates anti-nociceptive endocannabinoid signaling and promotes pro-nociceptive prostaglandin signaling. Accordingly, both acute nociception and its sensitization in chronic pain models are prevented by systemic or focal spinal inhibition of MGL activity. Despite its analgesic potential, the neurobiological substrates of beneficial MGL blockade have remained unexplored. Therefore, we examined the regional, cellular and subcellular distribution of MGL in spinal circuits involved in nociceptive processing. All immunohistochemical findings obtained with light, confocal or electron microscopy were validated in MGL-knockout mice. Immunoperoxidase staining revealed a highly concentrated accumulation of MGL in the dorsal horn, especially in superficial layers. Further electron microscopic analysis uncovered that the majority of MGL-immunolabeling is found in axon terminals forming either asymmetric glutamatergic or symmetric γ-aminobutyric acid/glycinergic synapses in laminae I/IIo. In line with this presynaptic localization, analysis of double-immunofluorescence staining by confocal microscopy showed that MGL colocalizes with neurochemical markers of peptidergic and non-peptidergic nociceptive terminals, and also with markers of local excitatory or inhibitory interneurons. Interestingly, the ratio of MGL-immunolabeling was highest in calcitonin gene-related peptide-positive peptidergic primary afferents, and the staining intensity of nociceptive terminals was significantly reduced in MGL-knockout mice. These observations highlight the spinal nociceptor synapse as a potential anatomical site for the analgesic effects of MGL blockade. Moreover, the presence of MGL in additional terminal types raises the possibility that MGL may play distinct regulatory roles in synaptic endocannabinoid or prostaglandin signaling according to its different cellular locations in the dorsal horn pain circuitry.

Introduction

To detect and minimize tissue damage, numerous signaling mechanisms operate together in the peripheral, spinal and supraspinal pain circuits (Basbaum *et al.*, 2009). Persistent noxious stimuli evoke various forms of molecular and cellular adaptations in these signaling processes (Sandkühler, 2009). Some may last beyond the resolution of tissue injury leading to chronic pain syndromes; a major conceptual and practical challenge for modern medicine, which requires a detailed understanding of how dynamic molecular changes are integrated into the cellular context of nociceptive processing in spinal and brain circuits (Kuner, 2010). However, the tremendous cellular complexity of the neuronal pain-processing circuitry (Todd, 2010) renders this task very difficult.

A promising development is the recent delineation of two interrelated signaling pathways with robust, but generally opposite, effects on nociception. Anti-nociceptive endocannabinoid signaling and pro-nociceptive prostaglandin signaling both regulate nociceptive transmission and its plasticity at specific anatomical locations (Reinold *et al.*, 2005; Agarwal *et al.*, 2007; Monory *et al.*, 2007; Vardeh *et al.*, 2009). Moreover, molecular components of these pathways exhibit region- and cell-type-specific quantitative changes in chronic pain models (Samad *et al.*, 2001; Zeilhofer, 2007; Sagar *et al.*, 2012; Simonetti *et al.*, 2013). Promoting endocannabinoid signaling or attenuating prostaglandin signaling are approaches generally considered to have analgesic potential (Zeilhofer & Brune, 2006; Jhaveri *et al.*, 2007). In fact, medical preparations from the cannabis plant stimulating cannabinoid (CB) receptors, and those from willow bark inhibiting prostaglandin-endoperoxidase synthases

Correspondence: Dr I. Katona, as above.
E-mail: katona@koki.hu

*E.H. and S.G.W. contributed equally to this study.

Received 26 September 2013, revised 29 November 2013, accepted 2 December 2013

© 2014 The Authors. *European Journal of Neuroscience* published by Federation of European Neuroscience Societies and John Wiley & Sons Ltd. This is an open access article under the terms of the Creative Commons Attribution License, which permits use, distribution and reproduction in any medium, provided the original work is properly cited.

(cyclooxygenases; COXs), are among the most ancient analgesic drugs used since antiquity.

An unexpected recent observation indicates that these two signaling pathways may be functionally linked by coordinated metabolism in the nervous system (Nomura *et al.*, 2008). Monoacylglycerol lipase (MGL) was first identified as a serine hydrolase inactivating the endocannabinoid 2-arachidonoylglycerol (2-AG) in the brain (Karlsson *et al.*, 1997; Dinh *et al.*, 2002; Blankman *et al.*, 2007). However, the resultant arachidonic acid pool can be further utilized by COXs to produce pro-nociceptive prostaglandins (Nomura *et al.*, 2011). Thus, MGL inhibition may have immense analgesic potential by facilitating anti-nociceptive 2-AG signaling and/or suppressing pro-nociceptive prostaglandin synthesis (Mulvihill & Nomura, 2013). Indeed, systemic administration of the selective MGL inhibitor 4-nitrophenyl-4-[bis(1,3-benzodioxol-5-yl)(hydroxy)methyl]piperidine-1-carboxylate (JZL184) suppresses thermal, visceral and noxious chemical pain (Long *et al.*, 2009; Schlosburg *et al.*, 2010; Busquets-Garcia *et al.*, 2011), and reduces mechanical and cold allodynia in neuropathic and inflammatory chronic pain (Kinsey *et al.*, 2009, 2010; Schlosburg *et al.*, 2010; Ghosh *et al.*, 2013). This anti-nociceptive effect may involve the regulation of endocannabinoid and/or prostaglandin signaling in the spinal nociceptive circuitry, because neuropathic pain increases spinal 2-AG levels and MGL expression (Wilkerson *et al.*, 2012; Guindon *et al.*, 2013). Moreover, direct spinal administration of JZL184 also efficiently reduces mechanically evoked or inflammation-induced nociceptive responses (Woodhams *et al.*, 2012).

Despite its apparent physiological and pathophysiological significance, direct evidence for the presence of MGL in neuronal components of the pain transmission pathway is lacking. Therefore, we aimed to investigate its regional and cellular distribution as well as its subcellular localization at different synapse types in the spinal nociceptive circuitry.

Materials and methods

Animals

Animal experiments were approved by the Hungarian Committee of the Scientific Ethics of Animal Research (license number: XIV-1-001/2332-4/2012), and were carried out according to the Hungarian Act of Animal Care and Experimentation (1998, XXVIII, Section 243/1998), which are in accordance with the European Communities Council Directive of 24 November 1986 (86⁄609⁄EEC; Section 243/1998). Littermate wild-type C57BL/6N mice (MGL+/+) and mice deficient in MGL (MGL−/−) (n = 17 and 18, respectively, 30–33 days old) were used in this study. The *mgll* gene was inactivated by deleting exon 3 containing the Ser-122 residue, a component of the catalytic triad for hydrolytic activity. Generation, breeding and genotyping of this line has been described in detail previously (Uchigashima *et al.*, 2011).

Perfusion and preparation of tissue sections

Mice were deeply anesthetized with a mixture of ketamine–xylazine (25 mg/mL ketamine, 5 mg/mL xylazine and 0.1 w/w% promethazine in H_2O; 1 mL per 100 g, i.p.). Animals were transcardially perfused with 0.9% saline for 2 min, followed by 100 mL of a fixative containing 4% paraformaldehyde (PFA) in 0.1 M phosphate buffer (PB; pH 7.4) for 20 min. After perfusion, the spinal cord was removed from the spinal column and post-fixed for 2 h in 4% PFA, then washed in 0.1 M PB. Fifty-micrometer transverse sections of the lumbar spinal cord were cut with a Leica VTS-1000 vibratome (Leica Microsystems, Wetzlar, Germany). All reagents were purchased either from Sigma-Aldrich Kft, Merck Kft, Roche Kft or Reanal Kft (all in Budapest, Hungary), unless otherwise stated.

Peroxidase-based immunohistochemistry

After slicing and several washing steps in 0.1 M PB, the spinal cord sections for peroxidase-based immunohistochemistry were incubated in 30% sucrose overnight, followed by freeze–thawing over liquid nitrogen four times to facilitate permeability within the tissue. Sections were washed extensively in 0.1 M PB to remove residual sucrose, and incubated for 10 min in 1% H_2O_2 in 0.1 M PB to block endogenous peroxidase activity. After washing in 0.1 M PB, sections were processed for immunoperoxidase reaction utilizing a standard protocol. All further washing steps and dilutions of the antibodies were performed in 0.05 M Tris-buffered saline (TBS; pH 7.4). Following extensive washing in TBS, sections were blocked in 1% human serum albumin (Sigma-Aldrich) for 2 h, then incubated with a polyclonal affinity-purified rabbit anti-MGL primary antibody (1 : 500; approximately 0.5 μg/mL) raised against the N-terminal 35 residues of the mouse MGL protein (Uchigashima *et al.*, 2011). Incubation was performed overnight at room temperature, then for a further 24 h at 4 °C. Specificity of the anti-MGL antibody was confirmed by the lack of immunostaining in spinal cord sections derived from MGL−/− mice, which were co-incubated within the same reaction wells throughout the entire process. After primary antibody incubation, the sections were washed in TBS three times and then incubated in biotinylated goat anti-rabbit IgG (1 : 400; Vector Laboratories, Burlingame, CA, USA) for 4 h. After washing, sections were kept in TBS at 4 °C overnight followed by an incubation with avidin-biotinylated horseradish peroxidase complex (1 : 500; Elite-ABC, Vector) for 3 h. After washing in TBS and then in Tris buffer (TB; 0.05 M, pH 7.6) twice, sections were incubated in the chromogen 3,3′-diaminobenzidine (DAB; 0.05% dissolved in TB) for 15 min in the dark. The immunoperoxidase reaction was initiated by addition of 0.01% H_2O_2 to the solution, and was terminated after approximately 15 min by changing the chromogen solution to TB. Sections were washed first in TB, and then extensively in PB, and finally stored in PB to await further processing.

Light microscopic analysis

For light microscopy, sections were briefly immersed in chromium gelatine [0.5% chromium (III) potassium sulfate dodecahydrate; Sigma-Aldrich] and mounted onto slides. After complete drying (approximately 60 min), slides were sequentially washed in Xylol I and II for 10 min each, covered with DePeX (Serva Electrophoresis GmbH, Heidelberg, Germany) and coverslipped. MGL-immunostaining was analysed with a Nikon Eclipse 80i microscope equipped with a Nikon DS-U2 digital camera using NIS-Elements Br software (Nikon Instruments). Digital images were processed with Adobe Photoshop CS5 software (Adobe Systems, San Jose, CA, USA). Images of sections from MGL+/+ and MGL−/− spinal cords incubated within the same well and mounted onto the same slide were merged into a single file. All *post hoc* image processing was performed simultaneously and identically for MGL+/+ and MGL−/− images, and no part of an image was modified separately.

Electron microscopic analysis

For electron microscopy, after development of the immunoperoxidase reaction, sections were first treated with 1% OsO_4 in 0.1 M PB

© 2014 The Authors. *European Journal of Neuroscience* published by Federation of European Neuroscience Societies and John Wiley & Sons Ltd.

for 10 min in the dark, on ice, and then dehydrated in an ascending series of ethanol solutions, followed by acetonitrile. An additional treatment with uranyl acetate (1% in 70% ethanol for 10 min in the dark, on ice) was included during the dehydration process. Sections were embedded in Durcupan (ACM, Fluka, Buchs, Switzerland). Areas of interest containing the dorsolateral fasciculus (Lissauer's tract) and the superficial laminae were cut from the dorsal horn of lumbar segments of both MGL+/+ and MGL−/− spinal cords, and re-sectioned to produce ultrathin 50-nm thin sections with a Leica EM UC6 Ultramicrotome (Leica Microsystems). These sections were collected on a Formvar-coated single-slot copper grid, contrasted with lead citrate (Ultrostain2; Leica), and examined with a Hitachi 7100 electron microscope (Hitachi High-Technologies, Tokyo, Japan). Electron micrographs at 40 000 × magnification were acquired with a Veleta CCD camera (Olympus Soft Imaging Solutions, Munster, Germany).

Double-immunofluorescence staining

To exclude a vague reported possibility of cross-reaction of the anti-MGL primary antibody with other primary antibodies when used in multiple immunofluorescence incubations, we followed a sequential immunostaining protocol as described earlier (Uchigashima *et al.*, 2011). All washing steps and antibody dilutions were performed in 0.05 M TBS (pH 7.4). After slicing and extensive washing, spinal cord sections containing the lumbar segments of MGL+/+ and MGL−/− mice were treated with a blocking solution containing 1% human serum albumin and 0.01% Triton X-100 in TBS (0.05 M, pH 7.4) for 2 h. Sections were then incubated with rabbit anti-MGL antibody (1 : 500) overnight at room temperature, followed by 24 h at 4 °C. Bound primary antibody was then detected by incubation with an Alexa Fluor 488-conjugated anti-rabbit secondary antibody (1 : 400; Jackson ImmunoResearch Europe, Suffolk, UK) for 5 h at room temperature. After several washing steps, a second blocking period was included with 10% normal rabbit serum (Vector) for 2 h. Subsequently, sections were incubated with one of the following antibodies as neurochemical markers of different axon terminal types: vesicular glutamate transporter 2 (vGluT2; polyclonal affinity-purified antibody raised in goat, 1 : 500, 0.4 μg/mL; Frontier Science, Hokkaido, Japan); vesicular inhibitory amino acid transporter (VIAAT; monoclonal affinity-purified antibody raised in mouse, 1 : 500, 2 μg/mL; Synaptic Systems, Goettingen, Germany); calcitonin gene-related peptide (CGRP; polyclonal antibody raised in sheep, 1 : 1000; Enzo Life Sciences, Farmingdale, NY, USA); or with the biotin-conjugated glycoprotein isolectin B4 (IB4) from *Bandeiraea simplicifolia* (L2140, 1 : 1000; Sigma). Primary antibody incubations were performed overnight at room temperature, followed by 24 h at 4 °C. After washing steps, immunostaining was visualized by using Alexa Fluor 594-conjugated species-specific secondary antibody treatment for 5 h at a dilution of 1 : 400, or with Alexa Fluor 594-conjugated streptavidin at a dilution of 1 : 200 for IB4 (all Jackson ImmunoResearch). Sections were then washed and stored in 0.1 M PB overnight, before mounting in Vectashield (Vector).

Antibody specificity

Specificity of the MGL-immunofluorescence staining examined in sections from MGL+/+ mice was validated by the almost complete absence of fluorescent signal in MGL−/− spinal cord sections. Very weak fluorescent puncta were scarcely detected, but this signal was not different to that seen when the primary anti-MGL antibody was omitted and MGL+/+ spinal cord sections were incubated with the fluorescent secondary antibody alone. Finally, further sequential staining experiments were also conducted in which the second primary antibody targeted to the given neurochemical marker was omitted. The absence of immunolabeling in these experiments excluded the possibility that false positive colocalization resulted from an interaction between the bound MGL antibody complex and the second fluorescent antibody, a situation that cannot be ruled out by using MGL−/− samples.

Full genetic deletion of vGluT2 produces a lethal phenotype *ex utero*, due to a lack of respiratory rhythm generation in the brainstem (Wallén-Mackenzie *et al.*, 2006), whilst deletion of VIAAT produces a lethal phenotype in which embryos die between E18.5 and birth (Wojcik *et al.*, 2006). Thus, unequivocal establishment of specificity of antibodies used to label vGluT2 or VIAAT is not feasible in the adult mouse spinal cord until cell-type-specific conditional knockout models become available. On the other hand, these antibodies are widely used to identify specific terminal types in the spinal cord and were used for this purpose in the present study, rather than to make specific observations about the respective proteins. Nevertheless, and despite the lack of available knockout controls, additional lines of evidence still suggest good target specificity of these antibodies. The goat polyclonal antibody directed against vGluT2 was generated with the same epitope and by using identical methods to an antibody raised in guinea pig (Miyazaki *et al.*, 2003). The two antibodies produce a similar characteristic vGluT2 staining pattern (Miura *et al.*, 2006), which could be entirely blocked by pre-incubation with the blocking peptide. The monoclonal mouse anti-VIAAT antibody, clone 117G4, has also been tested in numerous anatomical studies in combination with markers of other terminal types, and results in an entirely non-overlapping pattern to that seen with glutamatergic markers (Bogen *et al.*, 2006; Tafoya *et al.*, 2006; Baer *et al.*, 2007; Micheva *et al.*, 2010; Fan *et al.*, 2012; Hanson *et al.*, 2013). The sheep polyclonal antibody directed against CGRP produces the lamina I–IIo staining pattern characteristic of the laminar distribution of this neuropeptide in the rodent superficial spinal cord (Todd *et al.*, 2003). This staining pattern was entirely absent when the antiserum was pre-incubated with 10 nmol/mL CGRP, but not when incubated with the neuropeptides substance P or galanin. Moreover, this same characteristic CGRP-immunoreactivity in the superficial layers of the spinal cord is absent in CGRP knockout mice (Zhang *et al.*, 2001). The binding of the glycoprotein IB4 is generally considered to specifically visualize non-peptidergic primary afferent fibers in mammals (Silverman & Kruger, 1988; Snider & McMahon, 1998), and the biotin-conjugated form utilized here has also been widely used in previous anatomical studies to identify these neurons (Todd *et al.*, 2003; Zhao *et al.*, 2010; Wrobel *et al.*, 2011).

Confocal microscopic analysis

Images were obtained from the superficial dorsal horn with a Nikon A1R confocal laser-scanning system built on a Ti-E inverted microscope and operated by NIS-Elements AR 3.5 software. MG Argon Ion Laser (457–514 nm, 40 mW) and MG Yellow DPSS Laser (561 nm, 20 mW) were used as excitation lasers with appropriate filters for Alexa Fluor 488 and Alexa Fluor 594, respectively. Optimal confocal settings (laser power, gain, offset, pixel dwell, pixel size and confocal aperture) were initially determined on spinal cord sections derived from MGL+/+ mice, and have remained identical for all subsequent scans and images under each staining condition. Images were acquired in a sequential acquisition

© 2014 The Authors. *European Journal of Neuroscience* published by Federation of European Neuroscience Societies and John Wiley & Sons Ltd.

mode, and special care was taken to ensure that no pixels corresponding to any of the target proteins were saturated. Images were obtained by using a 1.4 NA 60 × CFI Plan Apochromat VC (Nikon) oil-immersion objective from a region of interest directly adjacent to the dorsolateral fasciculus (Lissauer's tract) in the medial portion of the dorsal horn. This area, corresponding to laminae I, IIo and a portion of IIi, comprised a 72 × 72 μm region in the center of the field of view (pixel size, 0.07 μm), and were rotated to lie parallel with the white matter border. Altogether 15 images were acquired at a z-separation of 0.15 μm, and starting at a depth of 4 μm from the upper surface of the section. For restoration of 3D image stacks, the Classical Maximum Likelihood Estimation algorithm in the Huygens deconvolution software (Scientific Volume Imaging, Hilversum, the Netherlands) was used. For each staining condition, fluorescence intensity threshold limits were then set to exclude background and maximize visibility of the specific signal. Identical thresholds were applied for each marker within each staining condition, and for MGL across all staining conditions.

Colocalization analysis

To ensure specificity and accuracy of colocalization quantification, all analyses were performed in parallel on both MGL+/+ and MGL−/− spinal cord sections. To measure the staining within and between genotypes, overall mean intensity values for the entire region of interest in the central optical section were determined for MGL, and for each of the markers, by ImageJ software (Mac Biophotonics, NIH, Bethesda, Maryland, USA). In each deconvolved optical stack, the colocalization ratios between the neuropeptide CGRP (a marker of peptidergic nociceptive primary afferents), IB4 (a marker of non-peptidergic nociceptive primary afferents), vGluT2 (a vesicular glutamate transporter found primarily in axon terminals of intrinsic excitatory interneurons) or VIAAT [a vesicular γ-aminobutyric acid (GABA)/glycine transporter found in axon terminals of intrinsic inhibitory interneurons] and MGL were assessed in randomly selected terminals. Altogether > 300 terminals of each type were analysed in three sections per animal, and in three animals per genotype. Boutons labeled with a terminal type-specific marker were selected in a single-channel image obtained from the center of the optical stack (approximately 5 μm from the surface of the section), and analysed by Adobe Photoshop CS5. A 6 × 6 grid of edge length of 12.5 μm was superimposed over each image, and one terminal was randomly selected within each box to ensure equal distribution of sampling in case of $vGluT_2$- and VIAAT-immunostainings, which cover the superficial laminae fairly homogenously. Because CGRP-immunostaining is only present in the upper half of the region of interest (LI–IIo), two profiles were selected from each box in the top three rows of the grid. Likewise, because IB4-binding terminals are only present in the lower half of the region of interest, the central portion of lamina II, two profiles were selected from each box in the bottom three rows of the grid. The MGL content of these randomly selected terminals was subsequently examined in a dual-color 3D projection throughout the entire optical stack in NIS-Elements. Assessment of the presence of a punctum representing MGL-immunolabeling was performed by visually examining the entire 3D extent of each terminal. Terminals possessing one or more MGL-immunofluorescent puncta falling entirely within the boundaries of the marker-defined bouton volume were considered to be MGL-positive. Puncta with any portion appearing outside the boundaries of the terminal were removed from the analysis sample, as were those falling within the first and last optical sections of the stack as deconvolution is not reliable at these positions. Percentage colocalization values for each marker were then calculated for each section and each animal, and then averaged. Data are expressed as mean ± SEM. The intra-terminal intensity of MGL staining for each of the 244 MGL-positive puncta was subsequently measured by ImageJ software. Terminals were selected from the center of unaltered deconvolved optical stacks, and the optical section in which the MGL-positive puncta were largest and most intense was identified. A region of interest encompassing the MGL-positive puncta was then selected. The mean intensity of staining was measured for each MGL-positive puncta. Data are expressed as arbitrary units and are the median ± interquartile range (IQR).

Statistical analysis

Potential increases in MGL-immunolabeling in CGRP-containing boutons vs. IB4-, or vGluT2- or VIAAT-positive axon terminals were assessed by one-tailed Mann–Whitney *U*-test followed by Bonferroni-correction, therefore an α-level of $P < 0.016$ was considered statistically significant. Potential differences in the intensity of CGRP-, IB4-, vGluT2- and VIAAT-staining between MGL+/+ and MGL−/− dorsal horn tissue were determined by the two-tailed Mann–Whitney *U*-test. An α-level of $P < 0.05$ was considered statistically significant.

Results

Regional distribution of MGL in the mouse spinal cord

To determine the spinal circuits in which MGL may play a regulatory role in 2-AG and/or prostaglandin signaling, the regional distribution pattern of MGL was first investigated by immunoperoxidase immunohistochemistry. The localization of MGL in lumbar spinal cord sections was visualized by a rabbit polyclonal antibody directed against the N-terminal 35 amino acids of MGL (Uchigashima *et al.*, 2011). The validity of the pattern of MGL-immunoreactivity was confirmed by co-incubating spinal cord sections from wild-type (MGL+/+) and knockout (MGL−/−) mice within the same reaction well throughout the entire staining process (Fig. 1A–D).

At the light microscopic level, a striking accumulation of dense MGL-positive immunostaining was detected in the dorsal horn of spinal cord sections derived from MGL+/+ mice (Fig. 1A). Conversely, MGL-immunoreactive precipitate was not visible in spinal cord sections derived from MGL−/− mice, confirming the specificity of the staining (Fig. 1B). A prominent and specific gradient in the intensity of MGL-immunostaining towards the superficial laminae was clearly visible within the dorsal horn. The strongest labeling was observed in lamina I–II with sparser labeling in deeper laminae (Fig. 1C–E). The level of MGL-immunostaining did not reach detection threshold in other regions of the spinal cord, for example around the central canal or in the ventral horn. Varying antibody concentrations or incubation times resulted in brown precipitate throughout the spinal cord; however, a similar staining intensity was observed in sections derived from MGL+/+ and MGL−/− mice (data not shown). A more sensitive antibody may reveal low levels of MGL in other spinal regions in the future, but this characteristic immunostaining pattern apparently predicts that the majority of the MGL enzyme is highly concentrated in neuronal and/or glial elements of the nociceptive circuitry in the superficial laminae of the dorsal horn.

© 2014 The Authors. *European Journal of Neuroscience* published by Federation of European Neuroscience Societies and John Wiley & Sons Ltd.

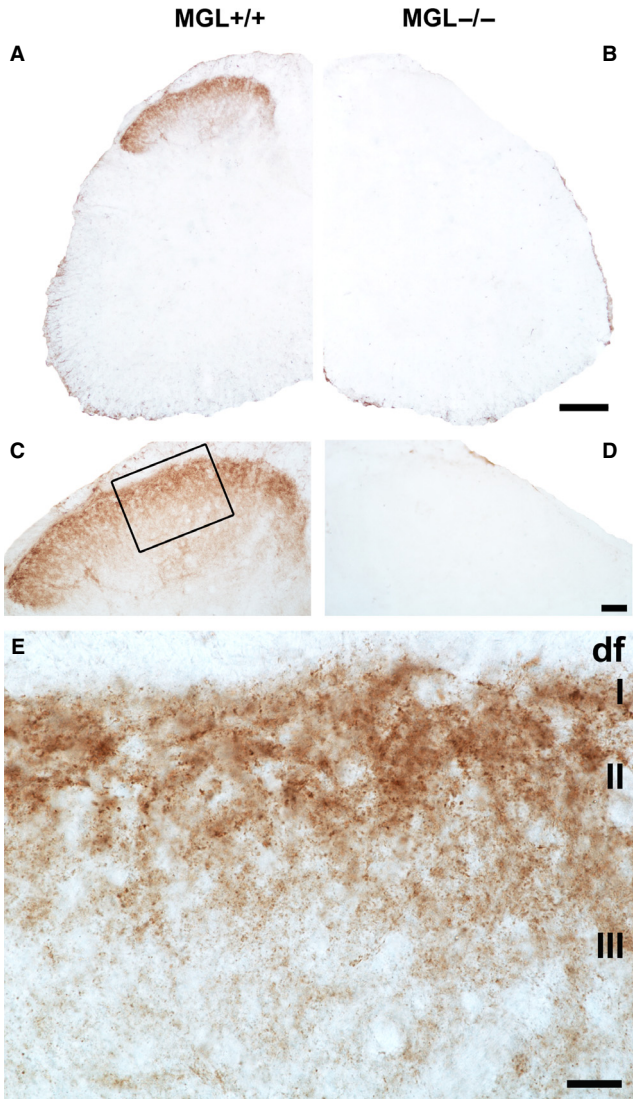

FIG. 1. Specific monoacylglycerol lipase (MGL)-immunoreactivity accumulates within the mouse lumbar superficial dorsal horn. (A and C) Light micrographs depict the distribution of the MGL protein, which is visualized via brown DAB precipitate formation at the site of immunoreaction. The pattern of MGL immunoreactivity was remarkably concentrated in the superficial laminae of the dorsal horn in an MGL+/+ mouse. Note that the staining remained below detection threshold in the ventral horn and around the central canal. (B and D) Specificity of the immunostaining was confirmed by the absence of the DAB precipitate in a spinal cord section derived from the MGL−/− knockout mouse. Importantly, the MGL+/+ and MGL−/− sections illustrated here were obtained from a littermate pair of animals, and were processed in parallel throughout the entire immunostaining and *post hoc* contrasting process. (E) A higher magnification light micrograph of the boxed region in (C) reveals the punctate nature of MGL-immunoreactivity throughout the superficial laminae, indicating expression in a restricted subset of subcellular compartments. Puncta of varying sizes and intensities may indicate expression in multiple such compartments. The dorsolateral funiculus ('df') contains very few MGL-positive profiles. In contrast, the majority of MGL-immunoreactivity is concentrated in lamina I (I) and lamina II (II) of Rexed, with staining intensity visibly decreasing towards deeper laminae, e.g. lamina III (III). Scale bars: 200 μm (A and B); 100 μm (C and D); 20 μm (E).

Presynaptic localization of MGL in excitatory and inhibitory axon terminals of the superficial dorsal horn

At higher magnification using light microscopy, the nature of the immunostaining pattern was also characteristic with high density of individual MGL-immunoreactive puncta of varying sizes and intensities (Fig. 1E). Larger and more strongly immunostained MGL-positive profiles were much more frequent in the superficial laminae especially in laminae I–II (Fig. 1E). This staining pattern was consistent across the medial and lateral aspects of the dorsal horn (Fig. 1C). These light microscopic observations indicate that the presence of MGL in cellular elements is highly compartmentalized within the termination zone of primary afferent neurons, an area in which expression of both the synthesizing enzyme of 2-AG, diacylglycerol lipase-α (DGL-α), and its major receptor target, the CB_1 receptor, are enriched (Nyilas *et al.*, 2009).

To elucidate which subcellular profiles MGL expression was concentrated in, spinal cord sections derived from MGL+/+ and MGL−/− mice with immunoperoxidase staining for MGL were further processed for analysis via electron microscopy. This high-resolution approach revealed that the vast majority of MGL-immunoreactivity in sections derived from MGL+/+ mice was confined within axon terminals in the superficial laminae of the dorsal horn (Figs 2 and 3). Importantly, the immunoreactive material was completely absent at the ultrastructural level in sections derived from MGL−/− mice (data not shown). In contrast to the predominantly presynaptic expression profile, postsynaptic structures like spine heads, smaller- or larger-sized dendritic shafts and cell bodies were always MGL-immunonegative (Figs 2 and 3). Consistent MGL-positive immunolabeling was observed only rarely in small-diameter structures, which may represent passing fibers or glial processes, structures that are not distinguishable at the ultrastructural level.

Interestingly, intense accumulation of MGL-immunoreactivity was primarily observed in axon terminals. However, these terminals represented several morphologically different types. The most prominent labeling was found in boutons forming asymmetrical synapses with a characteristic postsynaptic density in the postsynaptic profile (Fig. 2). These terminals presumably contain the excitatory neurotransmitter glutamate. Both large and small glutamatergic terminals were frequently found, which targeted larger dendritic shafts (Fig. $2A_1$ and A_2), but sometimes also smaller spine-like structures (Fig. $2B_1$ and B_2). On the other hand, despite a targeted analysis of synaptic glomeruli ($n = 43$) of both Type I and II in lamina II/III, none containing DAB precipitate in the central terminal was identified. Several other terminals that formed symmetrical, presumed GABA/glycinergic inhibitory synapses also turned out to be MGL-positive (Fig. 3). These boutons usually targeted larger-diameter dendritic shafts or sometimes formed symmetric synapses on the central terminal of a Type II glomerulus, demonstrating MGL-expression in axo-axonic inhibitory terminals (Fig. 3C).

Notably, many axon terminals were MGL-immunonegative (Fig. 3). These terminals were often found adjacent to MGL-immunopositive boutons, and formed both asymmetrical (Fig. $3A_1$ and A_2) as well as symmetrical synapses (Fig. $3B_1$ and B_2). The absence of immunolabeling may merely indicate that these terminals express MGL at levels below our detection threshold. However, the high density of DAB precipitate within labeled terminals was consistently present throughout several serial sections, whereas nearby MGL-immunonegative terminals consistently lacked DAB through all investigated sections. This likely suggests that the unlabeled terminals do not contain this serine hydrolase.

Taken together, these electron microscopic observations revealed that the majority of MGL is localized presynaptically in a heterogenous population of cellular elements within the spinal nociceptive circuitry.

© 2014 The Authors. *European Journal of Neuroscience* published by Federation of European Neuroscience Societies and John Wiley & Sons Ltd.

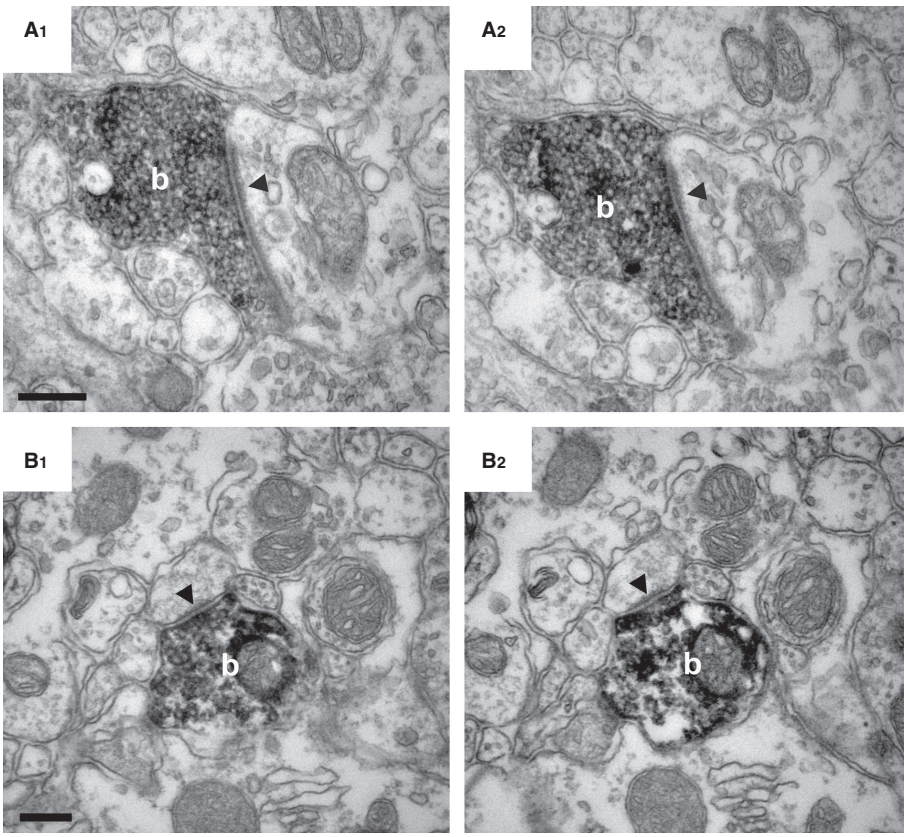

FIG. 2. MGL is presynaptically located in excitatory axon terminals in the superficial laminae of the mouse lumbar dorsal horn. (A and B) High-power electron micrographs demonstrate the presence of MGL in boutons ('b') forming asymmetric synapses (arrowheads) in the mouse superficial dorsal horn. MGL-immunoreactivity is represented by the black, electron-dense, DAB precipitate filling these terminals. The terminals are likely glutamatergic, based on the large postsynaptic density that is known to contain ionotropic glutamatergic receptors. Note the complete absence of MGL-immunoreactivity in the postsynaptic structures, which was consistent even when following the same bouton through consecutive sections (A_1 and A_2, and B_1 and B_2). Postsynaptic targets of MGL-positive axon terminals were variable from large-diameter dendritic shafts (A_1 and A_2) to small-diameter, putative dendritic spine heads (B_1 and B_2). Scale bars: 0.2 μm.

MGL is localized in CGRP-positive nociceptive primary afferents

To determine which extrinsic and/or intrinsic afferents of the nociceptive circuitry of the superficial dorsal horn carry presynaptic MGL, we utilized double-immunofluorescence staining and confocal microscopy. Given the earlier findings that direct spinal inhibition of MGL activity attenuates both acute and chronic forms of nociceptive signaling (Woodhams *et al.*, 2012), and endocannabinoid signaling mediates long-term depression of excitatory transmission on the spinal terminals of primary nociceptors (Kato *et al.*, 2012), we first investigated the presence of MGL at the initial central synapse of the nociceptive pathway. All primary afferent neurons terminating within the superficial dorsal horn are glutamatergic, and a significant proportion of those that carry capsaicin-sensitive nociceptive input co-express neuropeptides such as CGRP (Rosenfeld *et al.*, 1983; Wiesenfeld-Hallin *et al.*, 1984; Franco-Cereceda *et al.*, 1987). In fact, most nociceptive primary afferents in lamina I and IIo in rodents are thought to contain CGRP (Ju *et al.*, 1987). Thus, having observed MGL expression within excitatory axon terminals in these layers, we assessed the percentage of CGRP-positive profiles possessing MGL puncta within the superficial laminae of the medial dorsal horn. The region investigated comprised lamina I, IIo and a mid-portion of II, and thus constitutes the major termination zone of nociceptive primary afferent neurons (Todd, 2010).

In agreement with numerous previous reports, we observed a characteristic dense network of CGRP-immunofluorescent fibers especially in laminae I and IIo (Fig. 4A and B). In line with our observations utilizing an immunoperoxidase approach, the nature of MGL-positive fluorescent immunostaining consisted of a dense, punctate labeling pattern throughout the superficial dorsal horn of spinal cord sections derived from MGL+/+ mice (Fig. 4A). This staining pattern was almost entirely absent from MGL−/− sections, although a scarce residual background stain was still visible. Hence, colocalization analysis was performed on CGRP-positive terminal profiles from both MGL+/+ and MGL−/− tissue (n = 312, 3–3 animals). Numerous MGL-positive puncta of varying size and intensity were observed in CGRP-positive axon terminals in the superficial laminae of MGL+/+ spinal cord sections. A total of 127 MGL-immunofluorescent puncta was detected in a population of 81 of the assessed profiles, corresponding to an average colocalization ratio of 26 ± 4% (Fig. 4D). The majority of co-expressing structures contained a single MGL-immunopositive puncta, although a small population showed multiple intensely fluorescent profiles (Fig. 4C). All colocalization events were confirmed in all three dimensions to exclude that adjacent immunolabeling only visible from a single angle would result in false-positive colocalization values (Fig. 4C). A visible, but weak fluorescent signal was detectable only in a negligible minority of the selected terminals from MGL−/− tissue (3 ± 1%), validating the colocalization analysis performed in

© 2014 The Authors. *European Journal of Neuroscience* published by Federation of European Neuroscience Societies and John Wiley & Sons Ltd.

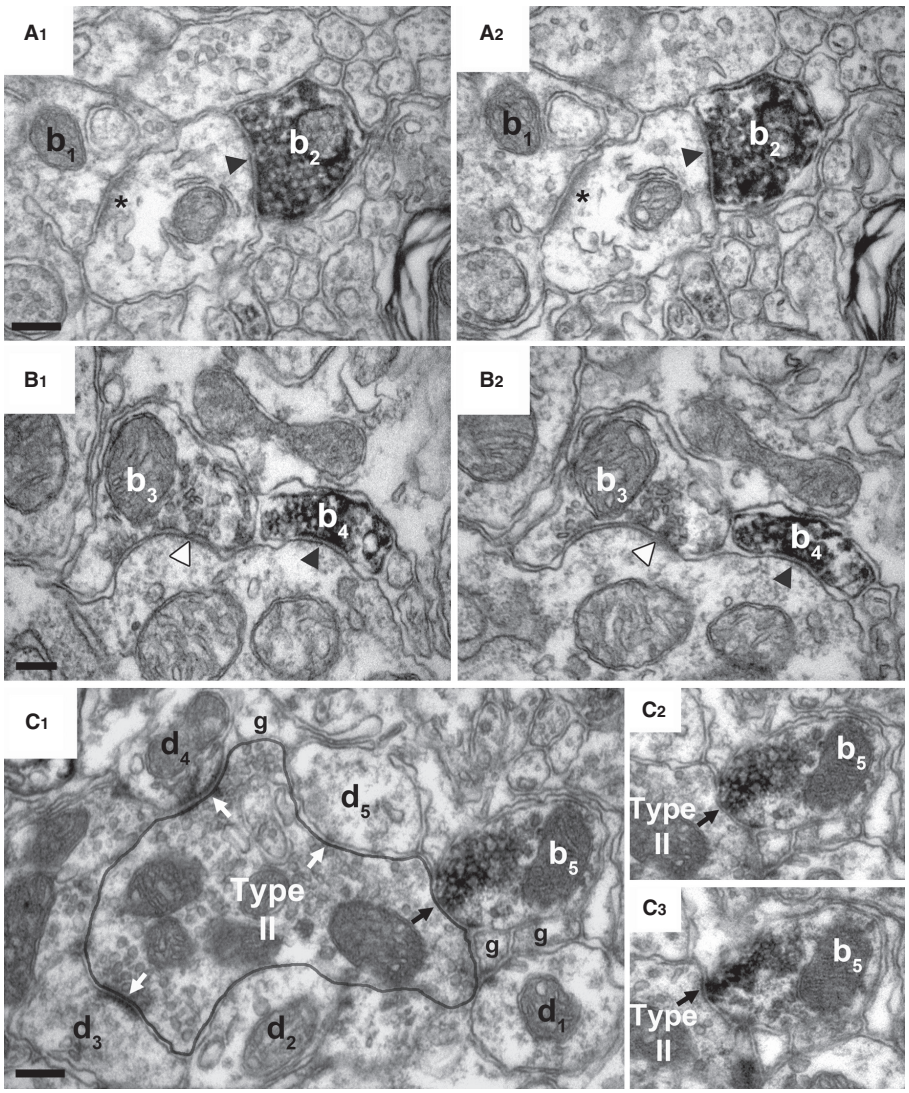

FIG. 3. Presynaptic localization of MGL in inhibitory axon terminals forming symmetrical synapses in the superficial laminae of the mouse lumbar dorsal horn. (A and B) High-power electron micrographs acquired from serial sections revealed high-density MGL-immunoreactivity in boutons (b_2 and b_4) terminating on MGL-immunonegative postsynaptic dendrites with symmetric, putative GABA/glycinergic synapses (black arrowhead). (A_1 and A_2) An MGL-immunonegative excitatory axon bouton (b_1) forming an asymmetric synapse (labeled by asterisk) is also shown, which indicates heterogeneity in the type of excitatory terminals carrying presynaptic MGL enzyme (see Fig. 2). (B_1 and B_2) Likewise, an MGL-immunonegative bouton (b_3) forming a symmetric synapse (white arrowhead) next to an MGL-positive bouton (b_4) suggests similar variability among inhibitory terminal types in the mouse superficial dorsal horn. (C_1) A further terminal type is illustrated in an electron micrograph depicting a Type II synaptic glomerulus, comprising a large central D-hair, non-nociceptive putative Aδ fiber and its multiple postsynaptic dendritic targets ($d_{1–5}$, white arrows). Whilst the central glutamatergic terminal is MGL-immunonegative, an adjacent MGL-immunopositive bouton (b_5) forms a putative GABA/glycinergic axo-axonic synapse (black arrow) onto the central D-hair Aδ terminal. (C_2 and C_3) Consecutive sections demonstrate the symmetrical nature of the axo-axonic synapse and confirm the dense accumulation of MGL-associated DAB within the bouton (b_5). The presence or absence of MGL-immunolabeling in a given pre- or postsynaptic profile was always consistent across all tested consecutive sections. Scale bars: 0.2 μm.

wild-type animals (Fig. 4D). Improved conditions for antibody binding (higher primary antibody concentration, enhanced tissue permeabilization and comparison of multiple blocking agents) were also tested in an attempt to attenuate the number of potential false-negative terminals. However, these attempts also reduced labeling specificity in parallel to increasing signal intensity, as determined in control knockout samples. Therefore, all reported colocalization ratios in the present study should be regarded as minimal estimations. Moreover, these observations highlight the mandatory use of knockout controls for each specific experiment, and for every subcellular compartment, if one aims to establish specific colocalization values.

Collectively, these experiments provided direct evidence that a significant population (at least approximately 23%) of peptidergic primary afferents contain the MGL enzyme in the superficial laminae of the dorsal horn.

MGL is expressed in a minor subset of IB4-binding, non-peptidergic primary afferent terminals

To determine whether MGL-immunoreactive profiles seen in lamina II might also correspond to MGL expression in the non-peptidergic population of nociceptive primary afferents, we next examined the

© 2014 The Authors. *European Journal of Neuroscience* published by Federation of European Neuroscience Societies and John Wiley & Sons Ltd.

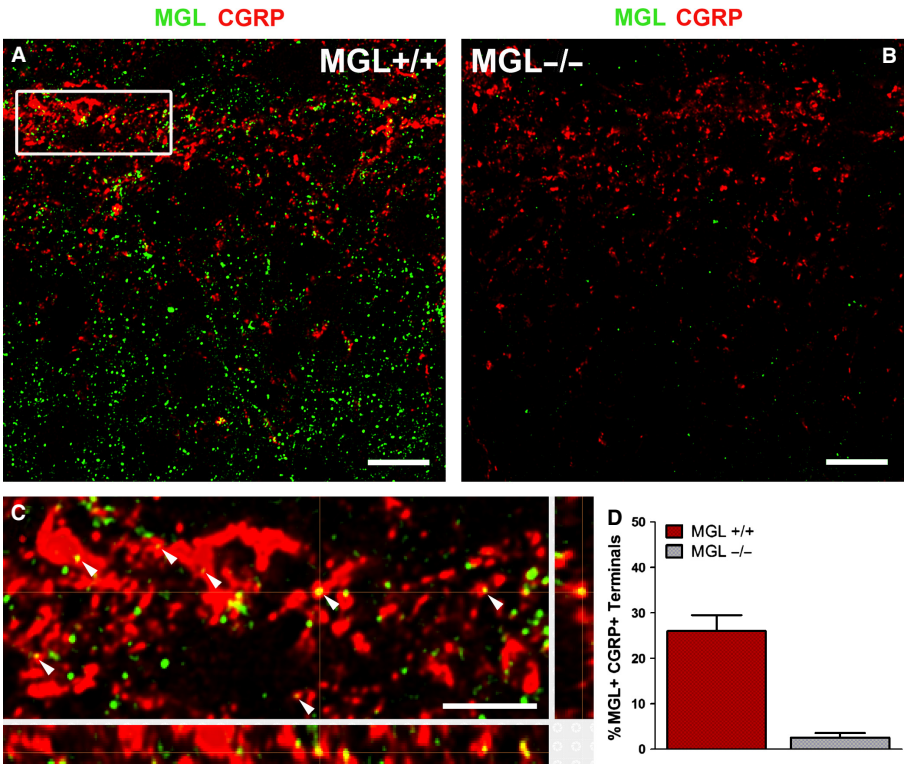

FIG. 4. Monoacylglycerol lipase (MGL) is present in calcitonin gene-related peptide (CGRP)-containing peptidergic primary afferents in the superficial laminae of the mouse lumbar dorsal horn. (A and B) Deconvolved confocal microscopy images of double-immunofluorescence staining reveal the distribution of MGL (green) and CGRP (red) in lamina I and II. Images were obtained from the center of 2-μm optical stacks from a region of interest in the medial lumbar dorsal horn of MGL+/+ (in A) and MGL−/− mice (in B). Note the characteristic lamina I–IIo concentration of CGRP-immunostaining in MGL+/+ mice, which is somewhat reduced in intensity in spinal cord sections derived from MGL−/− mice. In contrast, the dense MGL-immunostaining visible in the dorsal horn of MGL+/+ mice almost completely disappears in the MGL−/− spinal cord. (C) Magnified (500%) 3D reconstruction of the white boxed region depicted in (A), showing multiple profiles double-labeled for MGL and CGRP (arrowheads). Confirmation of colocalization is provided via the complete 3D optical reconstructions in the panels below and to the right of the main image panel. (D) Quantification of the percentage of CGRP-positive profiles also expressing MGL. Values obtained from MGL−/− spinal cord sections are also included as an indication of very low background levels of immunostaining. Scale bars: 10 μm (A and B); 2 μm (C).

colocalization of MGL with IB4. The binding of IB4 is generally considered to be a specific marker of non-peptidergic primary afferent fibers in mammals, and these neurons project their central terminals to the mid-portion of lamina II (Silverman & Kruger, 1988; Snider & McMahon, 1998).

Double-immunofluorescence studies revealed a very similar pattern of MGL-immunoreactivity to that observed previously in MGL+/+ tissue (Figs 4A and 5A). We also observed the characteristic, restricted pattern of IB4 binding largely confined to the mid-portion of lamina II (Fig. 5A). In contrast to the high level of colocalization seen between MGL and CGRP, far fewer double IB4-positive and MGL-immunopositive terminals were detected. In a randomly selected population of 318 IB4-positive profiles within the mid-portion of lamina II (n = 3 animals), only 28 MGL-immunofluorescent puncta were identified corresponding to an average colocalization ratio of 9 ± 1% (Fig. 5D). Only a single IB4-positive terminal with multiple MGL puncta was observed, and in general the puncta were of moderate intensity (Fig. 5C). In agreement with previous observations, only one of 323 terminals selected from MGL−/− tissue (n = 3 animals) contained a fluorescent signal (Fig. 5B), highlighting the specificity of immunostaining in these experiments. These observations demonstrate MGL protein expression in a small subset of non-peptidergic, primary afferent terminals, but suggest that the enzyme is much less abundant than in their peptidergic counterparts.

MGL is present in a small population of glutamatergic terminals derived from local interneurons in the superficial dorsal horn

Given the frequent occurrence of MGL-positive terminals forming asymmetrical synapses at the electron microscopic level, we next investigated the axon terminals of intrinsic glutamatergic interneurons. Spinal cord expression of vGluT2 is restricted to axon terminals, and predominantly to those found in lamina I and II of the lumbar dorsal horn (Todd *et al.*, 2003). Although not an exclusive marker for local glutamatergic interneurons, the few primary afferents positive for vGluT2 either contain weaker levels of this neurochemical marker than local excitatory terminals or are likely to be smaller in number compared with the high density of strong vGluT2-positive axon terminals (Todd *et al.*, 2003), which are generally considered to originate from local glutamatergic interneurons (Polgár *et al.*, 2010; Yasaka *et al.*, 2010).

In line with these reports, we observed a vGluT2-immunofluorescence labeling pattern consistent with axonal varicosities throughout the superficial dorsal horn (Fig. 6A and B). The distribution pattern of MGL-immunoreactivity was indistinguishable to that seen in previous experiments (Fig. 6A and B), and overall MGL-positive fluorescence intensity did not differ (data not shown). Colocalization analysis was performed on 319 vGluT2-positive axon terminals from MGL+/+ spinal cord sections, and on 323 vGluT2-positive boutons

© 2014 The Authors. *European Journal of Neuroscience* published by Federation of European Neuroscience Societies and John Wiley & Sons Ltd.

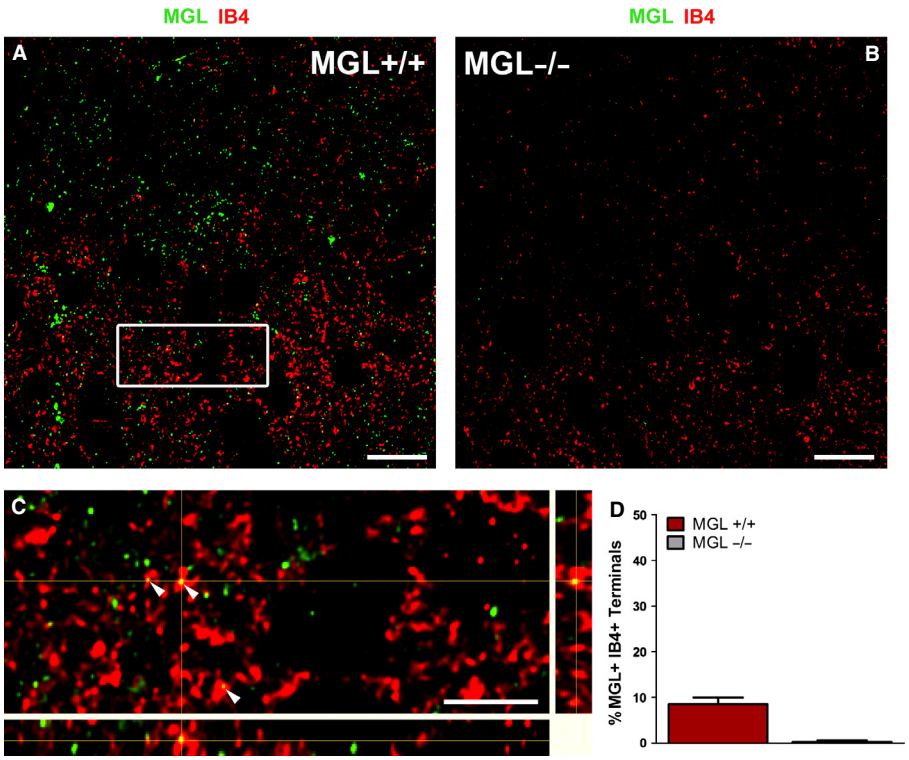

FIG. 5. Monoacylglycerol lipase (MGL) is present in a minority of isolectin B4 (IB4)-binding, non-peptidergic primary afferents in the superficial laminae of the mouse lumbar dorsal horn. (A and B) Deconvolved confocal microscopy images from sections double-stained for MGL (green) and IB4 (red), a marker of non-peptidergic, nociceptive primary afferent neurons, reveal little colocalization in the medial superficial dorsal horn. IB4-positive neurons terminate exclusively in the mid-portion of lamina II, thus labeled profiles seen in more superficial regions likely represent the passing axons of these cells. IB4-labeling is of notably greater intensity in MGL+/+ tissue (A) compared with MGL−/− tissue (B), although the overall staining pattern is similar. Specificity of MGL-labeling is indicated by the lack of immunofluorescence in MGL−/− tissue. (C) Enlarged magnification and 3D representation of the white boxed region depicted in (A), showing few profiles double-labeled for MGL and IB4 (arrowheads). The majority of IB4-positive profiles lack MGL-immunoreactivity. (D) Quantification of the percentage of IB4-positive profiles also expressing MGL. Values obtained from MGL−/− spinal cord sections are also included as an indication of the weak background labeling. Scale bars: 10 μm (A and B); 2 μm (C).

from MGL−/− sections (n = 3–3 animals). Interestingly, MGL-positive immunofluorescence signal was observed in only a minority of vGluT2-positive terminals. In total, 37 MGL-positive puncta were detected across 33 of the 319 terminals analysed, giving an average colocalization value of 10 ± 2% (Fig. 6D). A minor proportion of the selected terminals from MGL−/− sections displayed weak fluorescence signal (six out of 323 boutons; 2 ± 1%), which illustrates the very low level of background labeling. The intensity of MGL-immunostaining tended to be weak in vGluT2-containing terminals, and it was extremely rare to detect more than one punctum in a single terminal (Fig. 6C). In contrast, the few colocalizing MGL-positive terminals contained high levels of vGluT2-immunofluorescent signal (Fig. 6C). Thus, it appears that MGL is also present in a subset of intrinsic excitatory terminals (approximately 10%) in the superficial laminae of the dorsal horn.

MGL is expressed within a subset of inhibitory axon terminals in the superficial dorsal horn

Because terminals forming symmetrical synapses were also strongly labeled for MGL at the ultrastructural level, we next investigated the colocalization between MGL and the inhibitory amino acid transporter protein VIAAT. This neurochemical marker is a non-selective inhibitory amino acid transporter responsible for vesicular loading of both GABA and glycine in inhibitory axon terminals (Dumoulin *et al.*, 1999). As such, it can be used to visualize inhibitory axon terminals within neural tissue, including the spinal cord.

In the superficial dorsal horn, VIAAT-immunoreactivity was consistent with expression in axonal varicosities. In contrast to vGluT2-immunostaining, which was fairly homogenously distributed, the density of VIAAT-positive terminals was more prominent in lamina II than in lamina I (Fig. 7A and B). The distribution of MGL-positive immunofluorescent labeling was indistinguishable from previous experiments (Fig. 7A and B). Colocalization was assessed in a total of 321 and 323 terminals in spinal cord sections derived from MGL+/+ and MGL−/− mice, respectively (n = 3–3 animals). Altogether 52 MGL-positive fluorescent puncta were observed in 43 of the 321 terminals analysed, giving an average colocalization ratio of 13 ± 2% in GABA/glycinergic boutons. In contrast, only a negligible number of terminals were labeled in knockout sections (four out of 323 terminals, 1 ± 1%). The apparent heterogeneity in the laminar distribution of descending supraspinal GABAergic afferents, concentrated around lamina I–IIo (Antal *et al.*, 1996), was not matched by the homogeneous distribution of MGL-containing VIAAT-positive boutons observed here. Given that all primary afferent terminals are glutamatergic, if these GABAergic MGL-positive terminals are not supraspinal in origin it follows that they must belong to local inhibitory interneurons. Indeed, the vast majority of inhibitory lamina II interneurons give rise to dense local axon arbors also in lamina II (Yasaka *et al.*, 2010), and the MGL-positive axo-axonic terminals (Fig. 3C) are also supposed to derive from local parvalbumin-positive GABAergic cells (Hughes *et al.*, 2012). Thus, it seems likely that a subpopulation (approximately 12%) of local inhibitory interneurons express presynaptic MGL in their axon terminals.

© 2014 The Authors. *European Journal of Neuroscience* published by Federation of European Neuroscience Societies and John Wiley & Sons Ltd.

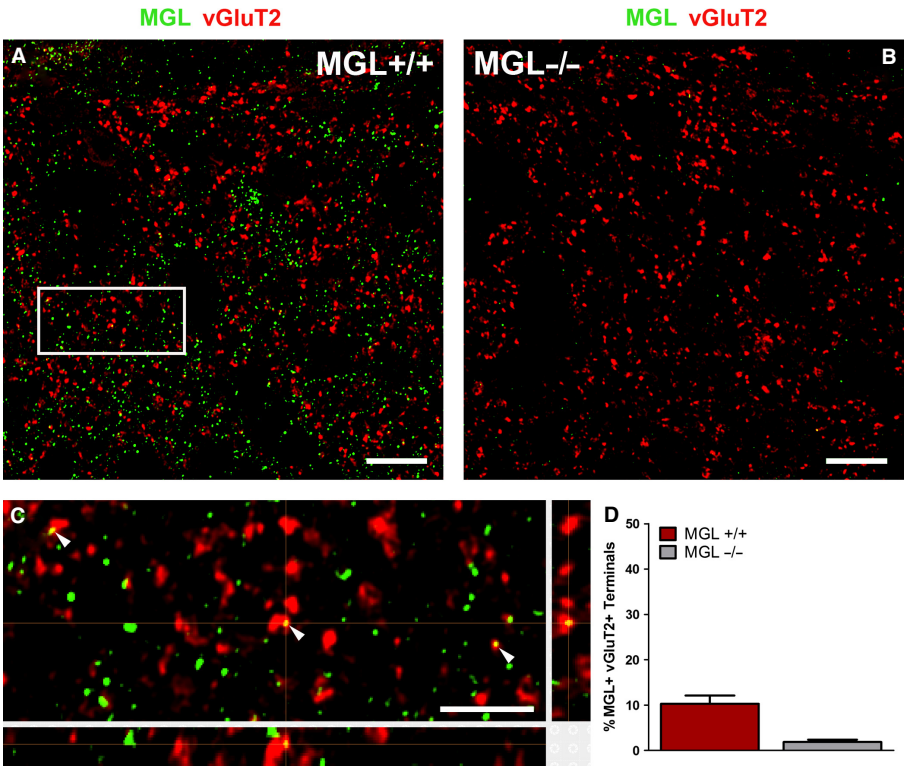

FIG. 6. Vesicular glutamate transporter 2 (vGluT2)-positive local excitatory terminals rarely contain monoacylglycerol lipase (MGL) in the superficial laminae of the mouse lumbar dorsal horn. (A) Deconvolved confocal microscopy images of MGL-immunofluorescence labeling (green) show a largely non-overlapping distribution pattern with vGluT2-immunostaining (red) in lamina I–II in the medial dorsal horn of MGL+/+ wild-type mice. vGluT2-immunoreactivity predominantly labels the axon terminals of intrinsic excitatory interneurons. (B) Whilst alterations in vGluT2-immunostaining were not discernible in spinal cord sections derived from MGL−/− mice, an almost complete absence of MGL-immunofluorescence was evident. (C) High-magnification of the white boxed region indicated in (A) shows occasional axon terminals, which contain both MGL and vGluT2 (arrowheads) as validated by 3D reconstruction analysis. Note that colocalization was observed in intensely labeled vGluT2-positive terminals, which are considered to belong to local excitatory interneurons. (D) Quantification of the percentage of vGluT2-immunofluorescent boutons, which are also immunopositive for MGL. Values obtained from MGL−/− sections are included as an indication of the low background levels of staining. Scale bars: 10 μm (A and B); 2 μm (C).

Taken together, the colocalization experiments revealed that MGL is mainly present in peptidergic primary afferents, but it is also found in a smaller subset of non-peptidergic primary afferents, as well as in intrinsic glutamatergic and GABA/glycinergic terminals.

MGL levels vary within different axon terminal populations

The observation that more CGRP-positive terminals contain MGL than other terminal types raises the possibility that MGL levels also vary in a synapse type-specific manner. To this end, MGL-immunolabeling in CGRP-positive boutons was compared with the other three bouton populations. The majority of terminals of all types contained only a single MGL punctum, but a number of both CGRP- and sometimes VIAAT-positive terminals were observed to have multiple immunofluorescent signals. This was significantly more frequent in the CGRP-positive population compared with IB4-positive terminals (one-tailed Mann–Whitney *U*-test with Bonferroni correction; $^{**}P = 0.002$) or in vGluT2-positive terminals (one-tailed Mann–Whitney test with Bonferroni correction; $^{*}P = 0.004$), but not in VIAAT-positive terminals (one-tailed Mann–Whitney *U*-test with Bonferroni correction; $P = 0.02$). The intensity of MGL-immunostaining was highly variable even between terminals of the same type. Individual intensity values for each MGL-positive puncta were measured in CGRP-positive terminals [median ± IQR: 449 ± 322 arbitrary units (AUs)], and revealed a significantly higher MGL-immunolabeling intensity compared with those measured within vGluT2-positive terminals (307 ± 367 U; one-tailed Mann–Whitney *U*-test with Bonferroni correction; $^{*}P = 0.006$). In contrast, the staining intensity of MGL-fluorescent puncta was not higher in the CGRP-positive terminals than those positive for IB4 (439 ± 308; one-tailed Mann–Whitney *U*-test with Bonferroni correction; $P = 0.3$) or VIAAT (494 ± 310; one-tailed Mann–Whitney *U*-test with Bonferroni correction; $P = 0.2$).

Genetic deletion of MGL results in the reduction of both CGRP-immunofluorescent and IB4-positive labeling intensity in the superficial dorsal horn

Previous findings suggested that MGL regulates axonal growth during neurodevelopment (Keimpema *et al.*, 2010). In addition, chronic pharmacological and genetic inactivation of MGL induces substantial changes in the efficacy of synaptic endocannabinoid signaling (Chanda *et al.*, 2010; Tanimura *et al.*, 2012). These observations raise the possibility that certain molecular or anatomical plasticity mechanisms shape the nociceptive circuitry in the dorsal horn of the MGL−/− mice, which would indicate a functional link between MGL and the activity of a given synapse type. To test this idea, intensity values for all four neurochemical markers were quantified from unaltered single images collected from the center of each optical stack and compared between the two genotypes (Fig. 8). Interestingly, median intensity values for CGRP-immunolabeling were significantly lower in spinal cord sections derived from MGL−/−

© 2014 The Authors. *European Journal of Neuroscience* published by Federation of European Neuroscience Societies and John Wiley & Sons Ltd.

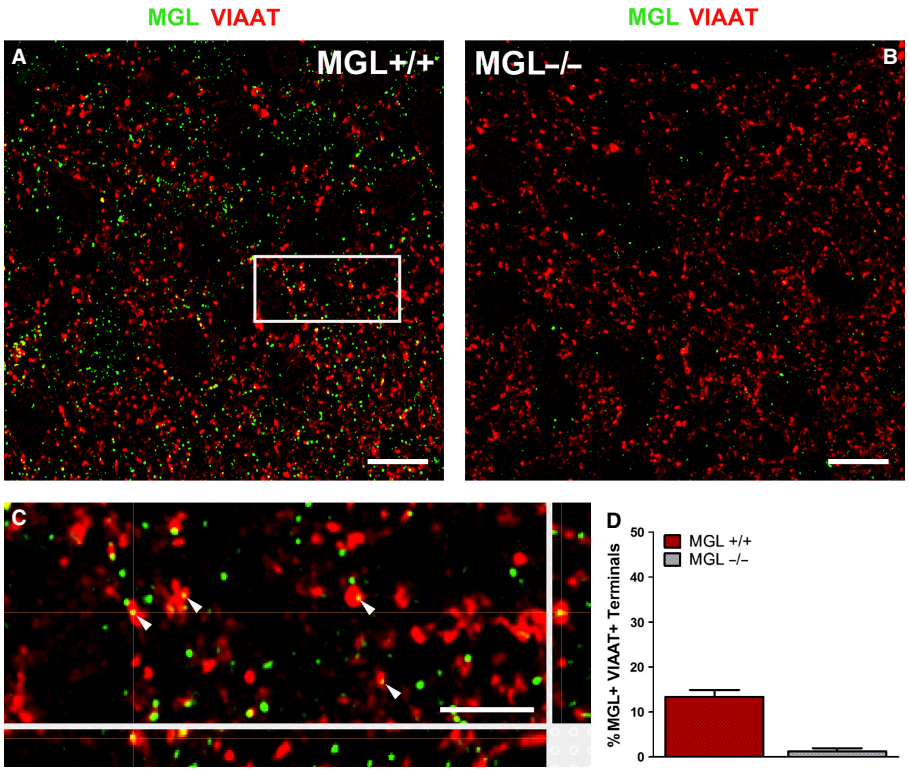

FIG. 7. Weak colocalization of monoacylglycerol lipase (MGL) and vesicular inhibitory amino acid transporter (VIAAT) in the superficial laminae of the mouse lumbar dorsal horn. (A) A deconvolved confocal image depicts double-immunofluorescence labeling for VIAAT (red) and MGL (green) in lamina I–II of a spinal cord section derived from an MGL+/+ mouse. MGL-immunofluorescence partially overlapped with the distribution of VIAAT, which is primarily a marker of local inhibitory axon terminals in these laminae. (B) MGL-immunostaining was largely absent in sections derived from MGL−/− knockout mice, but VIAAT-immunolabeling was not changed significantly. (C) A magnified 3D reconstruction of the white boxed region highlighted in (A) provided evidence for sparse colocalization of MGL and VIAAT (arrowheads). (D) Quantification of VIAAT-positive profiles, which contained MGL-immunolabeling resulted in a weak colocalization ratio. Values measured from MGL−/− sections demonstrate the low background levels of immunostaining. Scale bars: 10 μm (A and B); 2 μm (C).

mice than in sections from their MGL+/+ littermates (Fig. 8A; two-tailed Mann–Whitney *U*-test, median ± IQR: MGL+/+, 294 ± 104 AU; MGL−/−, 249 ± 56 AU; $*P = 0.03$, $n = 3$–3 animals). In addition, IB4-positive fluorescence intensity was also reduced in MGL−/− tissue (Fig. 8B; MGL+/+, 429 ± 166 AU; MGL−/−, 332 ± 102 AU; $**P = 0.006$, $n = 3$–3 animals). In contrast, no changes in the mean intensity of vGluT2-immunostaining (MGL+/+, 280 ± 138 AU; MGL−/− 265 ± 60 AU; $P = 0.86$, $n = 3$–3 animals) or VIAAT-immunostaining (MGL+/+, 205 ± 75 AU; MGL−/− 220 ± 80 AU; $P = 1$, $n = 3$–3 animals) were observed between genotypes (Fig. 8C and D). This somewhat unexpected observation demonstrates that chronic inactivation of MGL activity triggers an adaptive reorganization process in the central terminals of nociceptive primary afferent fibers.

Discussion

Inhibition of MGL, an enzymatic metabolic hub regulating both anti-nociceptive endocannabinoid signaling and pro-nociceptive prostaglandin signaling, is reportedly beneficial in several models of acute and chronic pain. In spite of its significance, the distribution of this enzyme has remained unexplored in pain circuits. Here we provide the first direct anatomical evidence for the presence of MGL in the mouse spinal nociceptive circuit, and report the following four major findings: (i) the regional distribution of MGL was highly concentrated in the superficial laminae of the dorsal horn, where most of the primary nociceptive afferents terminate and the majority of projection neurons are positioned; (ii) the subcellular localization of MGL was primarily confined to axon terminals indicating that MGL is in an ideal position to regulate endocannabinoid- and/or prostaglandin-mediated synaptic signaling in the dorsal horn; (iii) a substantial proportion of CGRP-positive primary nociceptive afferents contained MGL, and CGRP-immunostaining was significantly reduced following genetic deletion of MGL highlighting the spinal peptidergic nociceptor synapse as the anatomical location where MGL may primarily regulate nociception; (iv) MGL was also detected in subsets of non-peptidergic primary afferents as well as local excitatory and inhibitory terminals, which are involved in the processing of different aspects of nociceptive information. This heterogeneous presynaptic distribution of MGL in several neuronal elements of the nociceptive circuitry is consistent with the concept that its multiple enzymatic functions may vary at distinct synaptic localizations.

MGL abundance in the superficial laminae of the dorsal horn

The superficial laminae represent an anatomical hotspot where nociception can be most efficiently regulated (Todd, 2010). Most projection neurons are concentrated in lamina I of the dorsal horn, and are heavily involved in the transmission of acute nociceptive signals, and in the development of hyperalgesia in inflammatory and neuropathic pain states (Mantyh *et al.*, 1997; Nichols *et al.*, 1999). Lamina I and the underlying lamina II receive the majority of primary nociceptive and thermoceptive Aδ and C fiber afferents. Thus, the

© 2014 The Authors. *European Journal of Neuroscience* published by Federation of European Neuroscience Societies and John Wiley & Sons Ltd.

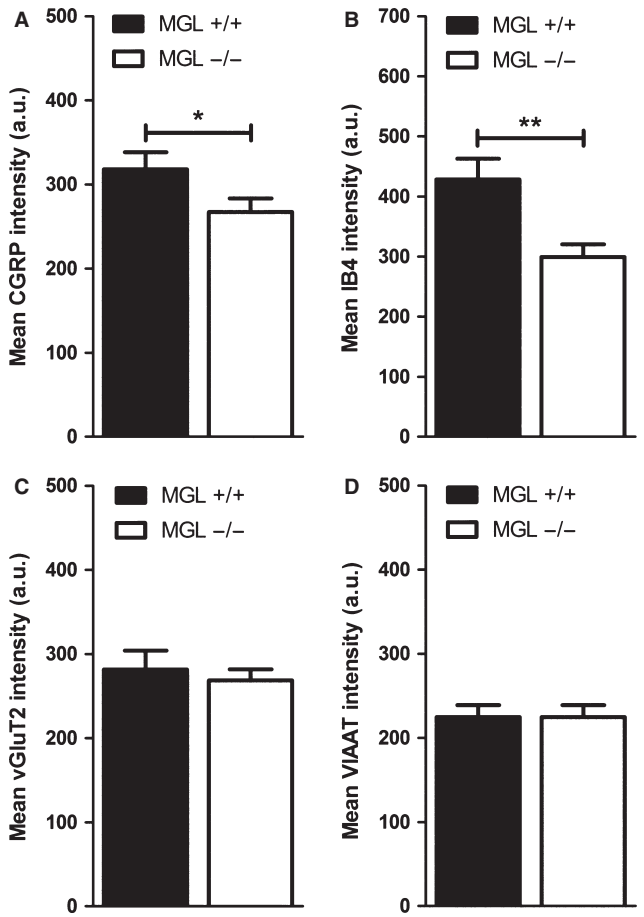

FIG. 8. Quantitative analysis of monoacylglycerol lipase (MGL)-immunostaining and immunofluorescence labeling for neurochemical markers in MGL+/+ wild-type and MGL−/− knockout mice. (A and B) Genetic deletion of MGL results in a significantly reduced calcitonin gene-related peptide (CGRP)-immunostaining and isolectin B4 (IB4)-labeling. (C and D) In contrast, vesicular glutamate transporter 2 (vGluT2)- or vesicular inhibitory amino acid transporter (VIAAT)-immunolabeling remained unaltered in the superficial dorsal horn of MGL−/− mice. Mean intensity values for (A) CGRP, (B) IB4, (C) vGluT2 and (D) VIAAT in the medial superficial dorsal horn of MGL+/+ vs. MGL−/− mice are presented. $*P = 0.03$, $**P = 0.006$, two-tailed Mann–Whitney *U*-test.

striking density gradient of MGL-immunoreactivity observed in lamina I and IIo is entirely consistent with the notion that MGL plays a prominent regulatory role in physiological and pathophysiological forms of nociception (Guindon & Hohmann, 2009). Notably, topical application of the selective MGL inhibitor JZL184 onto the dorsal horn potently suppresses both acute and inflammatory nociceptive activity in spinal neurons, an effect mediated by the CB_1 receptor (Woodhams *et al.*, 2012). The involvement of CB_1 receptors, the major target of the endocannabinoid 2-AG in the nervous system (Katona & Freund, 2008), suggests a regulatory role for MGL in nociception via termination of 2-AG signaling. In light of these functional data, it is particularly striking that both DGL-α, the synthesizing enzyme of 2-AG, and the CB_1 receptor share an exactly overlapping regional distribution with that of MGL in the superficial dorsal horn (Nyilas *et al.*, 2009).

Presynaptic MGL at spinal synapses

In contrast to the overlapping regional distribution pattern, the synthesizing and degrading enzymes of 2-AG display complementary synaptic distribution at the subcellular level. DGL-α was found exclusively in the somatodendritic domain of spinal neurons, most often located perisynaptically at the postsynaptic edge of metabotropic glutamate receptor 5 ($mGluR_5$)-containing excitatory synapses (Nyilas *et al.*, 2009). Conversely, in the present study the majority of MGL-immunoreactivity was found presynaptically in axon terminals throughout the superficial laminae. This presynaptic localization of MGL at spinal synapses is consistent with recent reports from other brain regions (Gulyás *et al.*, 2004; Ludányi *et al.*, 2011; Uchigashima *et al.*, 2011; Tanimura *et al.*, 2012), and suggests that MGL plays a conserved role in the regulation of synaptic endocannabinoid signaling throughout the CNS.

Genetic inactivation of DGL-α eliminates several forms of endocannabinoid-dependent synaptic plasticity in the brain, providing unequivocal evidence that 2-AG has a fundamental synaptic function (Gao *et al.*, 2010; Tanimura *et al.*, 2010; Yoshino *et al.*, 2011). Genetic or pharmacological blockade of MGL in the brain has an opposite effect, promoting 2-AG-mediated synaptic signaling processes (Pan *et al.*, 2009, 2011; Straiker *et al.*, 2009). These forms of synaptic plasticity all require presynaptically located CB_1 receptors (Kano *et al.*, 2009), which are also frequently found on axon terminals in the dorsal horn of the spinal cord (Hegyi *et al.*, 2009; Nyilas *et al.*, 2009). This canonical molecular organization ideally supports retrograde 2-AG signaling and seems to be a conserved feature of many synapses in the CNS, including the spinal cord (Katona & Freund, 2008).

This retrograde signaling pathway certainly has significance in various forms of nociception and nociceptive plasticity. For example, spinal 2-AG levels are increased in a non-opioid form of stress-induced analgesia (Suplita *et al.*, 2006). Stress-induced antinociception is facilitated by $mGluR_5$ activation, and requires both DGL-α and CB_1 activity (Nyilas *et al.*, 2009). Notably, direct spinal blockade of MGL has similar beneficial effects, which also require spinal CB_1 receptors (Suplita *et al.*, 2006). Taken together, these findings support the view that presynaptic MGL is integrated into the retrograde 2-AG signaling pathway at spinal synapses, thereby playing an important regulatory role in nociception.

The spinal nociceptor synapse: a potential anatomical site for the anti-nociceptive effects of MGL inhibition

Given the primarily anti-nociceptive effect of systemic and spinal MGL inhibition (Woodhams *et al.*, 2012; Mulvihill & Nomura, 2013), a major goal of the present study was to reveal the anatomical location(s) where MGL inhibition may suppress pain transmission in the dorsal horn nociceptive circuitry. Because the electron microscopic analysis revealed that MGL is mostly located in axon terminals, another set of experiments was dedicated to determine which of the major synapse types contain the highest density of MGL.

The highest colocalization ratio was observed in CGRP-positive primary afferents. These terminals target several cellular elements in the dorsal horn and, in parallel to their arborization in lamina II, they extensively innervate different types of lamina I projection neurons giving rise to ascending pathways, for example to the lateral parabrachial nucleus (Polgár *et al.*, 2010). These projection neurons are characterized by high expression levels of somatodendritic neurokinin 1 receptors, and their activity is facilitated by both substance P and CGRP released from a subset of primary afferents (Seybold, 2009). Thus, the presence of MGL in these nociceptive afferents supports the notion that MGL inhibition may control nociception at these spinal nociceptor synapses. Most importantly, a

© 2014 The Authors. *European Journal of Neuroscience* published by Federation of European Neuroscience Societies and John Wiley & Sons Ltd.

similar cell-type-specific knockout approach such as used for CB_1 receptor inactivation (Marsicano *et al.*, 2003; Agarwal *et al.*, 2007; Pernia-Andrade *et al.*, 2009) will be necessary to determine how MGL regulates endogenous analgesia at spinal nociceptor synapses *in vivo*.

Certainly, presynaptic CB_1 receptors on these nociceptors may also be critical for mediating anti-nociceptive 2-AG signaling. Interestingly, the ratio of CGRP-positive terminals containing MGL in the present study was in the same range as that reported recently, in terminals that colocalize substance P, CGRP and CB_1 receptors (Kato *et al.*, 2012). Furthermore, cell-type-specific deletion of CB_1 receptors provided direct evidence that retrograde endocannabinoid signaling mediates long-term depression of glutamatergic currents at these very same primary afferent terminals (Kato *et al.*, 2012), which have a surprisingly conserved evolutionary function at primary nociceptor synapses (Yuan & Burrell, 2013). Besides phasic endocannabinoid-mediated long-term depression as a candidate endogenous analgesic mechanism (Kato *et al.*, 2012), the involvement of tonic endocannabinoid signaling in the regulation of nociception may also be relevant. For example, two studies recently described downregulation of CB_1 receptors following chronic inactivation of MGL (Chanda *et al.*, 2010; Schlosburg *et al.*, 2010). Because this perturbation led to a functional tolerance for CB analgesic effects, it will therefore be interesting to investigate in the future whether such changes are also present in the spinal nociceptive circuitry, especially on peptidergic primary afferents.

Irrespective of the temporal dynamics of spinal endocannabinoid signaling, attenuation of glutamate release from nociceptive primary afferents is generally considered to suppress pain. Accordingly, activation of presynaptic CB_1 receptors on primary afferents reduces glutamate release from their terminals and consequently attenuates nociception (Kelly & Chapman, 2001; Morisset & Urban, 2001). These and many other studies collectively suggest that the 2-AG signaling pathway forms a tonic and/or phasic endogenous analgesic circuit by activating presynaptic CB_1 receptors at central nociceptor synapses (Chapman, 1999; Walker & Hohmann, 2005). These CB_1 receptors may therefore represent one target of beneficial action of CB preparations currently licensed to attenuate pain in cancer and multiple sclerosis (Pertwee, 2012). On the other hand, one also needs to take into consideration that the neurobiological substrate for this effect is certainly more complex (Agarwal *et al.*, 2007). For example, inhibition of MGL also contributes to distinct aspects of analgesia at supraspinal sites such as the periaqueductal gray matter and/or in the periphery (Hohmann *et al.*, 2005; Spradley *et al.*, 2010; Gregg *et al.*, 2012; Guindon *et al.*, 2013).

Heterogeneous distribution of MGL in various cellular elements of the nociceptive circuitry

The present finding that MGL, a regulator of at least two major brain signaling pathways (Mulvihill & Nomura, 2013), is located within at least four major synapse types supports the idea that this serine hydrolase may indeed play distinct physiological functions at different circuit locations. Moreover, the partial colocalization with neurochemical markers raises the possibility of further functional segregation of MGL into different subpopulations of primary afferents, intrinsic excitatory neurons or inhibitory terminals. For example, it will be crucial to study which of the four functionally distinct major inhibitory interneuron types in the dorsal horn contain presynaptic MGL (Polgár *et al.*, 2013). Our initial observations identified some MGL-positive inhibitory terminals forming axo-axonic synapses with Type II synaptic glomeruli, which may originate from the parvalbumin-positive interneuron population recently implicated in these connections (Hughes *et al.*, 2012). Interestingly, these axo-axonic synapses may represent a location at which MGL inhibition may facilitate tactile allodynia, rather than inducing a general analgesic effect. Moreover, postsynaptic target cell-specific quantitative differences in endocannabinoid-mediated plasticity are known in other brain regions (Peterfi *et al.*, 2012). Thus, future experiments could address whether the heterogeneity in endocannabinoid-mediated plasticity at spinal nociceptor synapses (Kato *et al.*, 2012) results from spatial segregation of MGL and CB_1 receptors into terminals innervating different postsynaptic target cell populations.

A circuit-specific contribution of MGL to the regulation of prostaglandins may also be relevant given the complexity of the molecular components of these pathways (Zeilhofer & Brune, 2006). Although pro-nociceptive prostaglandin E receptor 2 is located at specific GABAergic synapses in a cell-type-dependent manner (Ahmadi *et al.*, 2002; Reinold *et al.*, 2005), these receptors may also trigger glutamate release presynaptically (Sang *et al.*, 2005). To further complicate this picture, it is even possible for the same molecular pathway to play opposite roles in nociception, as exemplified by the reported pro-nociceptive role of CB_1 receptor signaling at spinal GABAergic synapses (Pernia-Andrade *et al.*, 2009), and the anti-nociceptive role of superficial spinal prostaglandin E receptor 3 (Nakamura *et al.*, 2000; Natura *et al.*, 2013), which implies that MGL inhibition may not even be anti-nociceptive at every circuit location.

Finally, another indication for the temporally and spatially complex functions of MGL in the spinal cord comes from the observation that both CGRP-immunoreactivity and IB4-labeling are downregulated in spinal cord sections from MGL−/− mice. This implies that MGL may play an important developmental function in the dorsal horn in accordance with earlier findings in other neuronal systems (Keimpema *et al.*, 2010). Activation of CB_1 receptors during axonal path finding *in vitro* causes growth cone repulsion and collapse (Berghuis *et al.*, 2007), and hyperactivity of the 2-AG-synthesizing enzyme DGL-α results in spherical exclusion of growth cones and diminishes cell–cell contact *in vitro* (Keimpema *et al.*, 2013). Deletion of MGL leads to a marked elevation in spinal cord 2-AG levels (Chanda *et al.*, 2010), and it is possible that this overspill of 2-AG produces similar effects *in vivo*. The observed reduction in CGRP-immunoreactivity and IB4-labeling may thus merely represent a developmental defect due to a loss of precise temporal and spatial control of 2-AG signaling during the critical period of primary afferent axonal targeting.

Conclusion

The neuronal circuitry of spinal nociceptive processing displays remarkable cellular and synaptic complexity (Todd, 2010). Contributing signaling pathways, such as the endocannabinoid system, fulfill multiple physiological functions at different circuit locations (Katona & Freund, 2012). The present anatomical findings demonstrating commensurate heterogeneous MGL distribution in the spinal dorsal horn therefore highlight the need for specific pre- and postsynaptic cell-type-specific approaches to elucidate the functional significance of endocannabinoid and prostaglandin signaling in different pain circuit components.

Acknowledgements

This work was primarily supported by a grant from Switzerland through the Swiss Contribution (SH/7/2/18), by the European Research Council Grant

© 2014 The Authors. *European Journal of Neuroscience* published by Federation of European Neuroscience Societies and John Wiley & Sons Ltd.

243153, by the Wellcome Trust International Senior Research Fellowship to I.K. (090946/Z/09/Z), and by the Momentum Program (LP2013-54/2013) of the Hungarian Academy of Sciences. We are grateful to Prof. Hanns Ulrich Zeilhofer and Carolin von Shoultz for discussions. We are also indebted to Erika Tischler, Balázs Pintér and Győző Goda for their excellent technical assistance, and to Barna Dudok for his advice on image processing and data analysis. We thank László Barna, the Nikon Microscopy Center at Institute of Experimental Medicine, Nikon Austria GmbH, and Auro-Science Consulting, Ltd, for kindly providing microscopy support. The authors declare no competing financial interests.

Abbreviations

2-AG, 2-arachidonoylglycerol; AU, arbitrary units; CB_1, cannabinoid receptor 1; CGRP, calcitonin gene-related peptide; COX, cyclooxygenase; DAB, 3,3′-diaminobenzidine; DGL-α, diacylglycerol lipase-alpha; GABA, γ-aminobutyric acid; IB4, plant isolectin B4; IQR, interquartile range; JZL184, 4-nitrophenyl-4-[bis(1,3-benzodioxol-5-yl)(hydroxy)methyl]piperidine-1-carboxylate; MGL, monoacylglycerol lipase; $mGluR_5$, metabotropic glutamate receptor 5; PB, phosphate buffer; PFA, paraformaldehyde; TB, Tris buffer; TBS, Tris-buffered saline; vGluT2, vesicular glutamate transporter 2; VIAAT, vesicular inhibitory amino acid transporter.

References

Agarwal, N., Pacher, P., Tegeder, I., Amaya, F., Constantin, C.E., Brenner, G.J., Rubino, T., Michalski, C.W., Marsicano, G., Monory, K., Mackie, K., Marian, C., Batkai, S., Parolaro, D., Fischer, M.J., Reeh, P., Kunos, G., Kress, M., Lutz, B., Woolf, C.J. & Kuner, R. (2007) Cannabinoids mediate analgesia largely via peripheral type 1 cannabinoid receptors in nociceptors. *Nat. Neurosci.*, **10**, 870–879.

Ahmadi, S., Lippross, S., Neuhuber, W.L. & Zeilhofer, H.U. (2002) PGE(2) selectively blocks inhibitory glycinergic neurotransmission onto rat superficial dorsal horn neurons. *Nat. Neurosci.*, **5**, 34–40.

Antal, M., Petkó, M., Polgár, E., Heizmann, C.W. & Storm-Mathisen, J. (1996) Direct evidence of an extensive GABAergic innervation of the spinal dorsal horn by fibres descending from the rostral ventromedial medulla. *Neuroscience*, **73**, 509–518.

Baer, K., Bürli, T., Huh, K.-H., Wiesner, A., Erb-Vögtli, S., Göckeritz-Dujmovic, D., Moransard, M., Nishimune, A., Rees, M.I., Henley, J.M., Fritschy, J.-M. & Fuhrer, C. (2007) PICK1 interacts with α7 neuronal nicotinic acetylcholine receptors and controls their clustering. *Mol. Cell. Neurosci.*, **35**, 339–355.

Basbaum, A.I., Bautista, D.M., Scherrer, G. & Julius, D. (2009) Cellular and molecular mechanisms of pain. *Cell*, **139**, 267–284.

Berghuis, P., Rajnicek, A.M., Morozov, Y.M., Ross, R.A., Mulder, J., Urbán, G.M., Monory, K., Marsicano, G., Matteoli, M., Canty, A., Irving, A.J., Katona, I., Yanagawa, Y., Rakic, P., Lutz, B., Mackie, K. & Harkany, T. (2007) Hardwiring the brain: endocannabinoids shape neuronal connectivity. *Science*, **316**, 1212–1216.

Blankman, J.L., Simon, G.M. & Cravatt, B.F. (2007) A comprehensive profile of brain enzymes that hydrolyze the endocannabinoid 2-arachidonoylglycerol. *Chem. Biol.*, **14**, 1347–1356.

Bogen, I.L., Boulland, J.-L., Mariussen, E., Wright, M.S., Fonnum, F., Kao, H.-T. & Walaas, S.I. (2006) Absence of synapsin I and II is accompanied by decreases in vesicular transport of specific neurotransmitters. *J. Neurochem.*, **96**, 1458–1466.

Busquets-Garcia, A., Puighermanal, E., Pastor, A., de la Torre, R., Maldonado, R. & Ozaita, A. (2011) Differential role of anandamide and 2-arachidonoylglycerol in memory and anxiety-like responses. *Biol. Psychiat.*, **70**, 479–486.

Chanda, P.K., Gao, Y., Mark, L., Btesh, J., Strassle, B.W., Lu, P., Piesla, M.J., Zhang, M.-Y., Bingham, B., Uveges, A., Kowal, D., Garbe, D., Kouranova, E.V., Ring, R.H., Bates, B., Pangalos, M.N., Kennedy, J.D., Whiteside, G.T. & Samad, T.A. (2010) Monoacylglycerol lipase activity is a critical modulator of the tone and integrity of the endocannabinoid system. *Mol. Pharmacol.*, **78**, 996–1003.

Chapman, V. (1999) The cannabinoid CB1 receptor antagonist, SR141716A, selectively facilitates nociceptive responses of dorsal horn neurones in the rat. *Brit. J. Pharmacol.*, **127**, 1765–1767.

Dinh, T.P., Carpenter, D., Leslie, F.M., Freund, T.F., Katona, I., Sensi, S.L., Kathuria, S. & Piomelli, D. (2002) Brain monoglyceride lipase participating in endocannabinoid inactivation. *Proc. Natl. Acad. Sci. USA*, **99**, 10819–10824.

Dumoulin, A., Rostaing, P., Bedet, C., Levi, S., Isambert, M.F., Henry, J.P., Triller, A. & Gasnier, B. (1999) Presence of the vesicular inhibitory amino acid transporter in GABAergic and glycinergic synaptic terminal boutons. *J. Cell Sci.*, **112**, 811–823.

Fan, K.Y., Baufreton, J., Surmeier, D.J., Chan, C.S. & Bevan, M.D. (2012) Proliferation of external globus pallidus-subthalamic nucleus synapses following degeneration of midbrain dopamine neurons. *J. Neurosci.*, **32**, 13718–13728.

Franco-Cereceda, A., Henke, H., Lundberg, J.M., Petermann, J.B., Hökfelt, T. & Fischer, J.A. (1987) Calcitonin gene-related peptide (CGRP) in capsaicin-sensitive substance P-immunoreactive sensory neurons in animals and man: distribution and release by capsaicin. *Peptides*, **8**, 399–410.

Gao, Y., Vasilyev, D.V., Goncalves, M.B., Howell, F.V., Hobbs, C., Reisenberg, M., Shen, R., Zhang, M.-Y., Strassle, B.W., Lu, P., Mark, L., Piesla, M.J., Deng, K., Kouranova, E.V., Ring, R.H., Whiteside, G.T., Bates, B., Walsh, F.S., Williams, G., Pangalos, M.N., Samad, T.A. & Doherty, P. (2010) Loss of retrograde endocannabinoid signaling and reduced adult neurogenesis in diacylglycerol lipase knock-out mice. *J. Neurosci.*, **30**, 2017–2024.

Ghosh, S., Wise, L.E., Chen, Y., Gujjar, R., Mahadevan, A., Cravatt, B.F. & Lichtman, A.H. (2013) The monoacylglycerol lipase inhibitor JZL184 suppresses inflammatory pain in the mouse carrageenan model. *Life Sci.*, **92**, 498–505.

Gregg, L.C., Jung, K.M., Spradley, J.M., Nyilas, R., Suplita, R.L. II, Zimmer, A., Watanabe, M., Mackie, K., Katona, I., Piomelli, D. & Hohmann, A.G. (2012) Activation of type 5 metabotropic glutamate receptors and diacylglycerol lipase-α initiates 2-arachidonoylglycerol formation and endocannabinoid-mediated analgesia. *J. Neurosci.*, **32**, 9457–9468.

Guindon, G. & Hohmann, A. (2009) The endocannabinoid system and pain. *CNS Neurol. Disord.-Dr.*, **8**, 18.

Guindon, J., Lai, Y., Takacs, S.M., Bradshaw, H.B. & Hohmann, A.G. (2013) Alterations in endocannabinoid tone following chemotherapy-induced peripheral neuropathy: effects of endocannabinoid deactivation inhibitors targeting fatty-acid amide hydrolase and monoacylglycerol lipase in comparison to reference analgesics following cisplatin treatment. *Pharmacol. Res.*, **67**, 94–109.

Gulyás, A.I., Cravatt, B.F., Bracey, M.H., Dinh, T.P., Piomelli, D., Boscia, F. & Freund, T.F. (2004) Segregation of two endocannabinoid-hydrolyzing enzymes into pre- and postsynaptic compartments in the rat hippocampus, cerebellum and amygdala. *Eur. J. Neurosci.*, **20**, 441–458.

Hanson, J.E., Deng, L., Hackos, D.H., Lo, S.-C., Lauffer, B.E., Steiner, P. & Zhou, Q. (2013) Histone deacetylase 2 cell autonomously suppresses excitatory and enhances inhibitory synaptic function in CA1 pyramidal neurons. *J. Neurosci.*, **33**, 5924–5929.

Hegyi, Z., Kis, G., Holló, K., Ledent, C. & Antal, M. (2009) Neuronal and glial localization of the cannabinoid-1 receptor in the superficial spinal dorsal horn of the rodent spinal cord. *Eur. J. Neurosci.*, **30**, 251–262.

Hohmann, A.G., Suplita, R.L., Bolton, N.M., Neely, M.H., Fegley, D., Mangieri, R., Krey, J.F., Walker, J.M., Holmes, P.V., Crystal, J.D., Duranti, A., Tontini, A., Mor, M., Tarzia, G. & Piomelli, D. (2005) An endocannabinoid mechanism for stress-induced analgesia. *Nature*, **435**, 1108–1112.

Hughes, D.I., Sikander, S., Kinnon, C.M., Boyle, K.A., Watanabe, M., Callister, R.J. & Graham, B.A. (2012) Morphological, neurochemical and electrophysiological features of parvalbumin-expressing cells: a likely source of axo-axonic inputs in the mouse spinal dorsal horn. *J. Physiol.*, **590**, 3927–3951.

Jhaveri, M.D., Richardson, D. & Chapman, V. (2007) Endocannabinoid metabolism and uptake: novel targets for neuropathic and inflammatory pain. *Brit. J. Pharmacol.*, **152**, 624–632.

Ju, G., Hokfelt, T., Brodin, E., Fahrenkrug, J., Fischer, J.A., Frey, P., Elde, R.P. & Brown, J.C. (1987) Primary sensory neurons of the rat showing calcitonin gene-related peptide immunoreactivity and their relation to substance P-, somatostatin-, galanin-, vasoactive intestinal polypeptide- and cholecystokinin-immunoreactive ganglion cells. *Cell Tissue Res.*, **247**, 417–431.

Kano, M., Ohno-Shosaku, T., Hashimotodani, Y., Uchigashima, M. & Watanabe, M. (2009) Endocannabinoid-mediated control of synaptic transmission. *Physiol. Rev.*, **89**, 309–380.

Karlsson, M., Contreras, J.A., Hellman, U., Tornqvist, H. & Holm, C. (1997) cDNA cloning, tissue distribution, and identification of the catalytic triad of monoglyceride lipase. *J. Biol. Chem.*, **272**, 27218–27223.

Kato, A., Punnakkal, P., Pernia-Andrade, A.J., von Schoultz, C., Sharopov, S., Nyilas, R., Katona, I. & Zeilhofer, H.U. (2012) Endocannabinoid-dependent plasticity at spinal nociceptor synapses. *J. Physiol.*, **590**, 4717–4733.

© 2014 The Authors. *European Journal of Neuroscience* published by Federation of European Neuroscience Societies and John Wiley & Sons Ltd.

Katona, I. & Freund, T.F. (2008) Endocannabinoid signaling as a synaptic circuit breaker in neurological disease. *Nat. Med.*, **14**, 923–930.
Katona, I. & Freund, T. (2012) Multiple functions of endocannabinoid signaling in the brain. *Annu. Rev. Neurosci.*, **35**, 529–558.
Keimpema, E., Barabas, K., Morozov, Y.M., Tortoriello, G., Torii, M., Cameron, G., Yanagawa, Y., Watanabe, M., Mackie, K. & Harkany, T. (2010) Differential subcellular recruitment of monoacylglycerol lipase generates spatial specificity of 2-arachidonoyl glycerol signaling during axonal pathfinding. *J. Neurosci.*, **30**, 13992–14007.
Keimpema, E., Alpar, A., Howell, F., Malenczyk, K., Hobbs, C., Hurd, Y.L., Watanabe, M., Sakimura, K., Kano, M., Doherty, P. & Harkany, T. (2013) Diacylglycerol lipase alpha manipulation reveals developmental roles for intercellular endocannabinoid signaling. *Sci. Rep.*, **3**, 2093.
Kelly, S. & Chapman, V. (2001) Selective cannabinoid CB1 receptor activation inhibits spinal nociceptive transmission *in vivo*. *J. Neurophysiol.*, **86**, 3061–3064.
Kinsey, S.G., Long, J.Z., O'Neal, S.T., Abdullah, R.A., Poklis, J.L., Boger, D.L., Cravatt, B.F. & Lichtman, A.H. (2009) Blockade of endocannabinoid-degrading enzymes attenuates neuropathic pain. *J. Pharmacol. Exp. Ther.*, **330**, 902–910.
Kinsey, S.G., Long, J.Z., Cravatt, B.F. & Lichtman, A.H. (2010) Fatty acid amide hydrolase and monoacylglycerol lipase inhibitors produce anti-allodynic effects in mice through distinct cannabinoid receptor mechanisms. *J. Pain*, **11**, 1420–1428.
Kuner, R. (2010) Central mechanisms of pathological pain. *Nat. Med.*, **16**, 1258–1266.
Long, J.Z., Li, W.W., Booker, L., Burston, J.J., Kinsey, S.G., Schlosburg, J.E., Pavon, F.J., Serrano, A.M., Selley, D.E., Parsons, L.H., Lichtman, A.H. & Cravatt, B.F. (2009) Selective blockade of 2-arachidonoylglycerol hydrolysis produces cannabinoid behavioral effects. *Nat. Chem. Biol.*, **5**, 37–44.
Ludányi, A., Hu, S.S.J., Yamazaki, M., Tanimura, A., Piomelli, D., Watanabe, M., Kano, M., Sakimura, K., Maglóczky, Z., Mackie, K., Freund, T.F. & Katona, I. (2011) Complementary synaptic distribution of enzymes responsible for synthesis and inactivation of the endocannabinoid 2-arachidonoylglycerol in the human hippocampus. *Neuroscience*, **174**, 50–63.
Mantyh, P.W., Rogers, S.D., Honore, P., Allen, B.J., Ghilardi, J.R., Li, J., Daughters, R.S., Lappi, D.A., Wiley, R.G. & Simone, D.A. (1997) Inhibition of hyperalgesia by ablation of lamina I spinal neurons expressing the substance P receptor. *Science*, **278**, 275–279.
Marsicano, G., Goodenough, S., Monory, K., Hermann, H., Eder, M., Cannich, A., Azad, S.C., Cascio, M.G., Gutierrez, S.O., van der Stelt, M., Lopez-Rodriguez, M.L., Casanova, E., Schütz, G., Zieglgansberger, W., Di Marzo, V., Behl., C. & Lutz, B. (2003) CB1 cannabinoid receptors and on-demand defense against excitotoxicity. *Science*, **302**, 84–88.
Micheva, K.D., Busse, B., Weiler, N.C., O'Rourke, N. & Smith, S.J. (2010) Single-synapse analysis of a diverse synapse population: proteomic imaging methods and markers. *Neuron*, **68**, 639–653.
Miura, E., Fukaya, M., Sato, T., Sugihara, K., Asano, M., Yoshioka, K. & Watanabe, M. (2006) Expression and distribution of JNK/SAPK-associated scaffold protein JSAP1 in developing and adult mouse brain. *J. Neurochem.*, **97**, 1431–1446.
Miyazaki, T., Fukaya, M., Shimizu, H. & Watanabe, M. (2003) Subtype switching of vesicular glutamate transporters at parallel fibre–Purkinje cell synapses in developing mouse cerebellum. *Eur. J. Neurosci.*, **17**, 2563–2572.
Monory, K., Blaudzun, H., Massa, F., Kaiser, N., Lemberger, T., Schütz, G., Wotjak, C.T., Lutz, B. & Marsicano, G. (2007) Genetic dissection of behavioural and autonomic effects of Δ9Tetrahydrocannabinol in mice. *PLoS Biol.*, **5**, e269.
Morisset, V. & Urban, L. (2001) Cannabinoid-induced presynaptic inhibition of glutamatergic EPSCs in substantia gelatinosa neurons of the rat spinal cord. *J. Neurophysiol.*, **86**, 40–48.
Mulvihill, M.M. & Nomura, D.K. (2013) Therapeutic potential of monoacylglycerol lipase inhibitors. *Life Sci.*, **92**, 492–497.
Nakamura, K., Kaneko, T., Yamashita, Y., Hasegawa, H., Katoh, H. & Negishi, M. (2000) Immunohistochemical localization of prostaglandin EP3 receptor in the rat nervous system. *J. Comp. Neurol.*, **421**, 543–569.
Natura, G., Bar, K.J., Eitner, A., Boettger, M.K., Richter, F., Hensellek, S., Ebersberger, A., Leuchtweis, J., Maruyama, T., Hofmann, G.O., Halbhuber, K.J. & Schaible, H.G. (2013) Neuronal prostaglandin E2 receptor subtype EP3 mediates antinociception during inflammation. *Proc. Natl. Acad. Sci. USA*, **110**, 13648–13653.
Nichols, M.L., Allen, B.J., Rogers, S.D., Ghilardi, J.R., Honore, P., Luger, N.M., Finke, M.P., Li, J., Lappi, D.A., Simone, D.A. & Mantyh, P.W. (1999) Transmission of chronic nociception by spinal neurons expressing the substance P receptor. *Science*, **286**, 1558–1561.
Nomura, D.K., Hudak, C.S.S., Ward, A.M., Burston, J.J., Issa, R.S., Fisher, K.J., Abood, M.E., Wiley, J.L., Lichtman, A.H. & Casida, J.E. (2008) Monoacylglycerol lipase regulates 2-arachidonoylglycerol action and arachidonic acid levels. *Bioorg. Med. Chem. Lett.*, **18**, 5875–5878.
Nomura, D.K., Morrison, B.E., Blankman, J.L., Long, J.Z., Kinsey, S.G., Marcondes, M.C., Ward, A.M., Hahn, Y.K., Lichtman, A.H., Conti, B. & Cravatt, B.F. (2011) Endocannabinoid hydrolysis generates brain prostaglandins that promote neuroinflammation. *Science*, **334**, 809–813.
Nyilas, R., Gregg, L.C., Mackie, K., Watanabe, M., Zimmer, A., Hohmann, A.G. & Katona, I. (2009) Molecular architecture of endocannabinoid signaling at nociceptive synapses mediating analgesia. *Eur. J. Neurosci.*, **29**, 1964–1978.
Pan, B., Wang, W., Long, J.Z., Sun, D., Hillard, C.J., Cravatt, B.F. & Liu, Q.-S. (2009) Blockade of 2-arachidonoylglycerol hydrolysis by selective monoacylglycerol lipase inhibitor 4-nitrophenyl 4-(Dibenzo[d][1,3]dioxol-5-yl(hydroxy)methyl)piperidine-1-carboxylate (JZL184) enhances retrograde endocannabinoid signaling. *J. Pharmacol. Exp. Ther.*, **331**, 591–597.
Pan, B., Wang, W., Zhong, P., Blankman, J.L., Cravatt, B.F. & Liu, Q.-S. (2011) Alterations of endocannabinoid signaling, synaptic plasticity, learning, and memory in monoacylglycerol lipase knock-out mice. *J. Neurosci.*, **31**, 13420–13430.
Pernia-Andrade, A.J., Kato, A., Witschi, R., Nyilas, R., Katona, I., Freund, T.F., Watanabe, M., Filitz, J., Koppert, W., Schuttler, J., Ji, G., Neugebauer, V., Marsicano, G., Lutz, B., Vanegas, H. & Zeilhofer, H.U. (2009) Spinal endocannabinoids and CB1 receptors mediate C-fiber-induced heterosynaptic pain sensitization. *Science*, **325**, 760–764.
Pertwee, R.G. (2012) Targeting the endocannabinoid system with cannabinoid receptor agonists: pharmacological strategies and therapeutic possibilities. *Philos. T. Roy. Soc. B.*, **367**, 3353–3363.
Peterfi, Z., Urban, G.M., Papp, O.I., Nemeth, B., Monyer, H., Szabo, G., Erdelyi, F., Mackie, K., Freund, T.F., Hajos, N. & Katona, I. (2012) Endocannabinoid-mediated long-term depression of afferent excitatory synapses in hippocampal pyramidal cells and GABAergic interneurons. *J. Neurosci.*, **32**, 14448–14463.
Polgár, E., Al Ghamdi, K.S. & Todd, A.J. (2010) Two populations of neurokinin 1 receptor-expressing projection neurons in lamina I of the rat spinal cord that differ in AMPA receptor subunit composition and density of excitatory synaptic input. *Neuroscience*, **167**, 1192–1204.
Polgár, E., Sardella, T.C.P., Tiong, S.Y.X., Locke, S., Watanabe, M. & Todd, A.J. (2013) Functional differences between neurochemically-defined populations of inhibitory interneurons in the rat spinal dorsal horn. *Pain*, **154**, 2606–2615.
Reinold, H., Ahmadi, S., Depner, U.B., Layh, B., Heindl, C., Hamza, M., Pahl, A., Brune, K., Narumiya, S., Muller, U. & Zeilhofer, H.U. (2005) Spinal inflammatory hyperalgesia is mediated by prostaglandin E receptors of the EP2 subtype. *J. Clin. Invest.*, **115**, 673–679.
Rosenfeld, M.G., Mermod, J.J., Amara, S.G., Swanson, L.W., Sawchenko, P.E., Rivier, J., Vale, W.W. & Evans, R.M. (1983) Production of a novel neuropeptide encoded by the calcitonin gene via tissue-specific RNA processing. *Nature*, **304**, 129–135.
Sagar, D.R., Burston, J.J., Woodhams, S.G. & Chapman, V. (2012) Dynamic changes to the endocannabinoid system in models of chronic pain. *Philos. T. Roy. Soc. B.*, **367**, 3300–3311.
Samad, T.A., Moore, K.A., Sapirstein, A., Billet, S., Allchorne, A., Poole, S., Bonventre, J.V. & Woolf, C.J. (2001) Interleukin-1beta-mediated induction of Cox-2 in the CNS contributes to inflammatory pain hypersensitivity. *Nature*, **410**, 471–475.
Sandkühler, J. (2009) Models and mechanisms of hyperalgesia and allodynia. *Physiol. Rev.*, **89**, 707–758.
Sang, N., Zhang, J., Marcheselli, V., Bazan, N.G. & Chen, C. (2005) Postsynaptically synthesized prostaglandin E2 (PGE2) modulates hippocampal synaptic transmission via a presynaptic PGE2 EP2 receptor. *J. Neurosci.*, **25**, 9858–9870.
Schlosburg, J.E., Blankman, J.L., Long, J.Z., Nomura, D.K., Pan, B., Kinsey, S.G., Nguyen, P.T., Ramesh, D., Booker, L., Burston, J.J., Thomas, E.A., Selley, D.E., Sim-Selley, L.J., Liu, Q.S., Lichtman, A.H. & Cravatt, B.F. (2010) Chronic monoacylglycerol lipase blockade causes functional antagonism of the endocannabinoid system. *Nat. Neurosci.*, **13**, 1113–1119.
Seybold, V.S. (2009) The role of peptides in central sensitization. In Canning, B.J. & Spina, D. (Eds), *Sensory Nerves*. Springer, Berlin, Heidelberg, pp. 451–491.
Silverman, J.D. & Kruger, L. (1988) Lectin and neuropeptide labeling of separate populations of dorsal root ganglion neurons and associated

© 2014 The Authors. *European Journal of Neuroscience* published by Federation of European Neuroscience Societies and John Wiley & Sons Ltd.

"nociceptor" thin axons in rat testis and cornea whole-mount preparations. *Somatosens. Res.*, **5**, 259–267.
Simonetti, M., Hagenston, A.M., Vardeh, D., Freitag, H.E., Mauceri, D., Lu, J., Satagopam, V.P., Schneider, R., Costigan, M., Bading, H. & Kuner, R. (2013) Nuclear calcium signaling in spinal neurons drives a genomic program required for persistent inflammatory pain. *Neuron*, **77**, 43–57.
Snider, W.D. & McMahon, S.B. (1998) Tackling pain at the source: new ideas about nociceptors. *Neuron*, **20**, 629–632.
Spradley, J.M., Guindon, J. & Hohmann, A.G. (2010) Inhibitors of monoacylglycerol lipase, fatty-acid amide hydrolase and endocannabinoid transport differentially suppress capsaicin-induced behavioral sensitization through peripheral endocannabinoid mechanisms. *Pharmacol. Res.*, **62**, 249–258.
Straiker, A., Hu, S.S.-J., Long, J.Z., Arnold, A., Wager-Miller, J., Cravatt, B.F. & Mackie, K. (2009) Monoacylglycerol lipase limits the duration of endocannabinoid-mediated depolarization-induced suppression of excitation in autaptic hippocampal neurons. *Mol. Pharmacol.*, **76**, 1220–1227.
Suplita, R.L., Gutierrez, T., Fegley, D., Piomelli, D. & Hohmann, A.G. (2006) Endocannabinoids at the spinal level regulate, but do not mediate, nonopioid stress-induced analgesia. *Neuropharmacology*, **50**, 372–379.
Tafoya, L.C.R., Mameli, M., Miyashita, T., Guzowski, J.F., Valenzuela, C.F. & Wilson, M.C. (2006) Expression and function of SNAP-25 as a universal SNARE component in GABAergic neurons. *J. Neurosci.*, **26**, 7826–7838.
Tanimura, A., Yamazaki, M., Hashimotodani, Y., Uchigashima, M., Kawata, S., Abe, M., Kita, Y., Hashimoto, K., Shimizu, T., Watanabe, M., Sakimura, K. & Kano, M. (2010) The endocannabinoid 2-arachidonoylglycerol produced by diacylglycerol lipase α mediates retrograde suppression of synaptic transmission. *Neuron*, **65**, 320–327.
Tanimura, A., Uchigashima, M., Yamazaki, M., Uesaka, N., Mikuni, T., Abe, M., Hashimoto, K., Watanabe, M., Sakimura, K. & Kano, M. (2012) Synapse type-independent degradation of the endocannabinoid 2-arachidonoylglycerol after retrograde synaptic suppression. *Proc. Natl. Acad. Sci. USA*, **109**, 12195–12200.
Todd, A.J. (2010) Neuronal circuitry for pain processing in the dorsal horn. *Nat. Rev. Neurosci.*, **11**, 823–836.
Todd, A.J., Hughes, D.I., Polgár, E., Nagy, G.G., Mackie, M., Ottersen, O.P. & Maxwell, D.J. (2003) The expression of vesicular glutamate transporters VGLUT1 and VGLUT2 in neurochemically defined axonal populations in the rat spinal cord with emphasis on the dorsal horn. *Eur. J. Neurosci.*, **17**, 13–27.
Uchigashima, M., Yamazaki, M., Yamasaki, M., Tanimura, A., Sakimura, K., Kano, M. & Watanabe, M. (2011) Molecular and morphological configuration for 2-arachidonoylglycerol-mediated retrograde signaling at mossy cell & granule cell synapses in the dentate gyrus. *J. Neurosci.*, **31**, 7700–7714.
Vardeh, D., Wang, D., Costigan, M., Lazarus, M., Saper, C.B., Woolf, C.J., Fitzgerald, G.A. & Samad, T.A. (2009) COX2 in CNS neural cells mediates mechanical inflammatory pain hypersensitivity in mice. *J. Clin. Invest.*, **119**, 287–294.
Walker, J.M. & Hohmann, A.G. (2005) Cannabinoid mechanisms of pain suppression. *Handb. Exp. Pharmacol.*, **168**, 509–554.
Wallén-Mackenzie, Å., Gezelius, H., Thoby-Brisson, M., Nygård, A., Enjin, A., Fujiyama, F., Fortin, G. & Kullander, K. (2006) Vesicular glutamate transporter 2 is required for central respiratory rhythm generation but not for locomotor central pattern generation. *J. Neurosci.*, **26**, 12294–12307.
Wiesenfeld-Hallin, Z., Hökfelt, T., Lundberg, J.M., Forssmann, W.G., Reinecke, M., Tschopp, F.A. & Fischer, J.A. (1984) Immunoreactive calcitonin gene-related peptide and substance P coexist in sensory neurons to the spinal cord and interact in spinal behavioral responses of the rat. *Neurosci. Lett.*, **52**, 199–204.
Wilkerson, J.L., Gentry, K.R., Dengler, E.C., Wallace, J.A., Kerwin, A.A., Armijo, L.M., Kuhn, M.N., Thakur, G.A., Makriyannis, A. & Milligan, E.D. (2012) Intrathecal cannabilactone CB2R agonist, AM1710, controls pathological pain and restores basal cytokine levels. *Pain*, **153**, 1091–1106.
Wojcik, S.M., Katsurabayashi, S., Guillemin, I., Friauf, E., Rosenmund, C., Brose, N. & Rhee, J.-S. (2006) A shared vesicular carrier allows synaptic corelease of GABA and glycine. *Neuron*, **50**, 575–587.
Woodhams, S.G., Wong, A., Barrett, D.A., Bennett, A.J., Chapman, V. & Alexander, S.P.H. (2012) Spinal administration of the monoacylglycerol lipase inhibitor JZL184 produces robust inhibitory effects on nociceptive processing and the development of central sensitization in the rat. *Brit. J. Pharmacol.*, **167**, 1609–1619.
Wrobel, L., Schorscher-Petcu, A., Dupré, A., Yoshida, M., Nishimori, K. & Tribollet, E. (2011) Distribution and identity of neurons expressing the oxytocin receptor in the mouse spinal cord. *Neurosci. Lett.*, **495**, 49–54.
Yasaka, T., Tiong, S.Y.X., Hughes, D.I., Riddell, J.S. & Todd, A.J. (2010) Populations of inhibitory and excitatory interneurons in lamina II of the adult rat spinal dorsal horn revealed by a combined electrophysiological and anatomical approach. *Pain*, **151**, 475–488.
Yoshino, H., Miyamae, T., Hansen, G., Zambrowicz, B., Flynn, M., Pedicord, D., Blat, Y., Westphal, R.S., Zaczek, R., Lewis, D.A. & Gonzalez-Burgos, G. (2011) Postsynaptic diacylglycerol lipase mediates retrograde endocannabinoid suppression of inhibition in mouse prefrontal cortex. *J. Physiol.*, **589**, 4857–4884.
Yuan, S. & Burrell, B.D. (2013) Non-nociceptive afferent activity depresses nocifensive behavior and nociceptive synapses via an endocannabinoid-dependent mechanism. *J. Neurophysiol.*, **110**, 2607–2616.
Zeilhofer, H.U. (2007) Prostanoids in nociception and pain. *Biochem. Pharmacol.*, **73**, 165–174.
Zeilhofer, H.U. & Brune, K. (2006) Analgesic strategies beyond the inhibition of cyclooxygenases. *Trends Pharmacol. Sci.*, **27**, 467–474.
Zhang, L., Hoff, A.O., Wimalawansa, S.J., Cote, G.J., Gagel, R.F. & Westlund, K.N. (2001) Arthritic calcitonin/alpha calcitonin gene-related peptide knockout mice have reduced nociceptive hypersensitivity. *Pain*, **89**, 265–273.
Zhao, J., Lee, M.-C., Momin, A., Cendan, C.-M., Shepherd, S.T., Baker, M.D., Asante, C., Bee, L., Bethry, A., Perkins, J.R., Nassar, M.A., Abrahamsen, B., Dickenson, A., Cobb, B.S., Merkenschlager, M. & Wood, J.N. (2010) Small RNAs control sodium channel expression, nociceptor excitability, and pain thresholds. *J. Neurosci.*, **30**, 10860–10871.

© 2014 The Authors. *European Journal of Neuroscience* published by Federation of European Neuroscience Societies and John Wiley & Sons Ltd.